Regulation of type 2 innate lymphoid cell–dependent airway hyperreactivity by butyrate

Christina Li-Ping Thio, MS,[a,b] Po-Yu Chi, MS,[b] Alan Chuan-Ying Lai, PhD,[b] and Ya-Jen Chang, PhD[a,b] *Taipei, Taiwan*

GRAPHICAL ABSTRACT

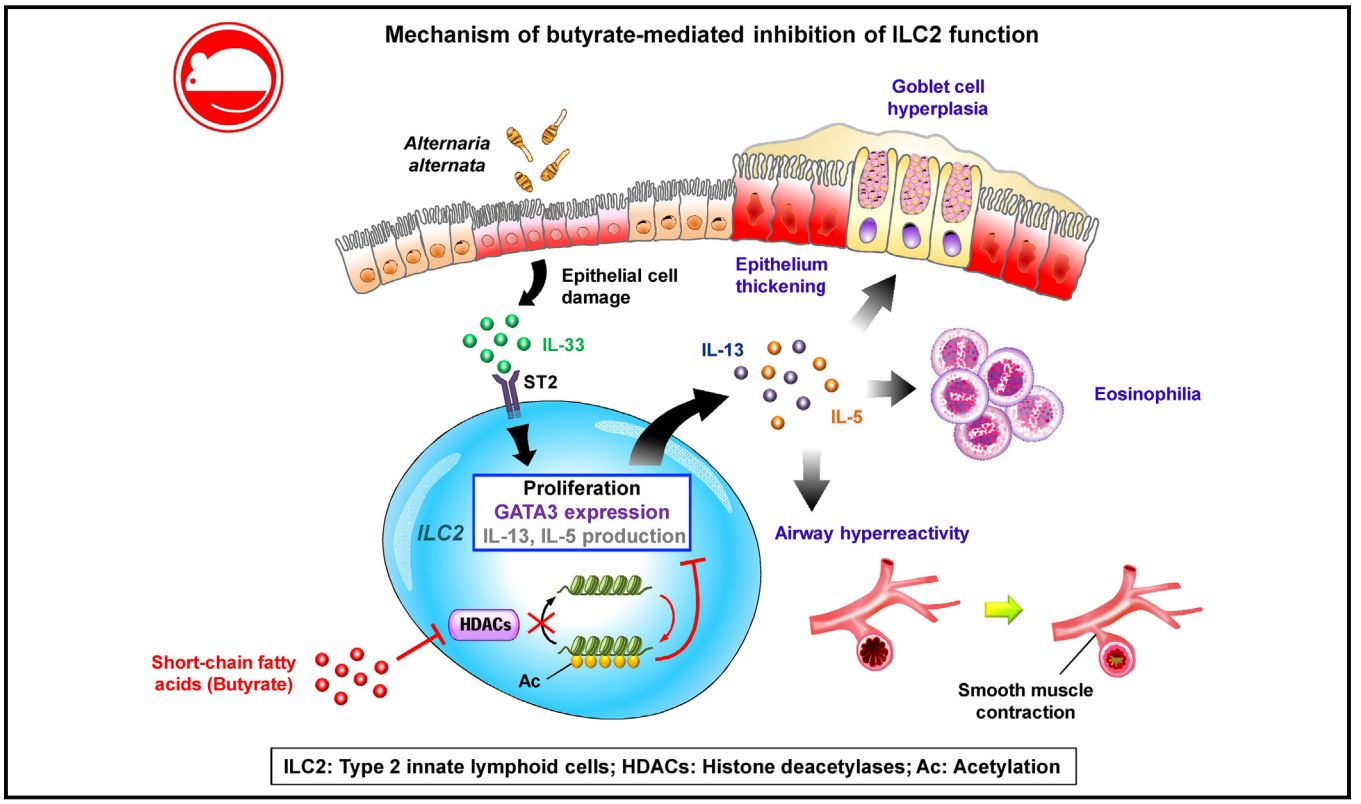

Background: Allergic asthma is characterized by airway hyperreactivity (AHR) and inflammation driven by aberrant T_H2 responses. Type 2 innate lymphoid cells (ILC2s) are a critical source of the T_H2 cytokines IL-5 and IL-13, which promote acute asthma exacerbation. Short-chain fatty acids (SCFAs) have been shown to attenuate T cell–mediated allergic airway inflammation. However, their role in regulation of ILC2-driven AHR and lung inflammation remains unknown.
Objective: We investigated the immunomodulatory role of SCFAs in regulation of ILC2-induced AHR and airway inflammation and delineated the mechanism involved.
Methods: We assessed the role of SCFAs in regulating survival, proliferation, and cytokine production in lung sorted ILC2s. The SCFA butyrate was administered through drinking water or intranasally in BALB/c mice to evaluate its role in the ILC2-driven inflammatory response in IL-33 and *Alternaria alternata* models of allergic inflammation. We further confirmed our findings in human ILC2s.
Results: We show that butyrate, but not acetate or propionate, inhibited IL-13 and IL-5 production by murine ILC2s. Systemic and local administration of butyrate significantly ameliorated ILC2-driven AHR and airway inflammation. We further demonstrate that butyrate inhibited ILC2 proliferation and GATA3 expression but did not induce cell apoptosis, likely through histone deacetylase (HDAC) inhibition, because trichostatin A, a pan-HDAC inhibitor, exerted similar effects on

From [a]the Taiwan International Graduate Program (TIGP) in Molecular Medicine, National Yang-Ming University and Academia Sinica, and [b]the Institute of Biomedical Sciences, Academia Sinica, Taipei.

Supported in part by the Ministry of Science and Technology (105-2628-B-001-009-MY3 and 105-2320-B-001-001 to Y.-J.C.) and by the Academia Sinica Career Development Award (104-CDA-L05 to Y.-J.C.) in Taiwan.
Disclosure of potential conflict of interest: Y.-J. Chang reports grant funding from the Ministry of Science & Technology (MOST) and a career development award from Academia Sinica. The rest of the authors declare that they have no relevant conflicts of interest.

Received for publication September 5, 2017; revised January 19, 2018; accepted for publication February 17, 2018.
Corresponding author: Ya-Jen Chang, PhD, Institute of Biomedical Sciences, Academia Sinica, No. 128 Academia Road, Section 2, Nankang, Taipei, Taiwan 11529. E-mail: yajchang@ibms.sinica.edu.tw.
0091-6749/$36.00

https://doi.org/10.1016/j.jaci.2018.02.032

ILC2s. Importantly, cotreatment with trichostatin A and butyrate did not result in an additive effect. Finally, we show that butyrate reduces cytokine production in human ILC2s. Conclusion: Our findings identify butyrate as a critical regulator of ILC2 proliferation and function through its HDAC inhibitory activity and can serve as a potential therapeutic target for asthma. (J Allergy Clin Immunol 2018;■■■:■■■-■■■.)

Key words: *Short-chain fatty acids, butyrate, type 2 innate lymphoid cells, allergic asthma, eosinophilic airway inflammation*

Abbreviations used
AHR: Airway hyperreactivity
BALF: Bronchoalveolar lavage fluid
ERK: Extracellular signal-regulated kinase
Foxp3: Forkhead box p3
FVD: Fixable viability dye
GPR: G-coupled protein receptor
HDAC: Histone deacetylase
ICOS: Inducible costimulator
ILC: Innate lymphoid cell
ILC2: Type 2 innate lymphoid cell
NF-κB: Nuclear factor κB
PI: Propidium iodide
PMA: Phorbol 12-myristate 13-acetate
Rag2: Recombination-activating gene 2
SCFA: Short-chain fatty acid
TSA: Trichostatin A
TCR: T-cell receptor
Treg: Regulatory T

Allergic asthma is a chronic inflammatory condition associated with hypersensitivity to inhaled antigens and is driven by aberrant innate and adaptive immune responses. The cardinal features of allergic asthma include mucus hypersecretion, pulmonary eosinophilic infiltration, and airway hyperreactivity (AHR). Long-term airway remodeling is also observed in patients with chronic asthma.[1,2] There is an unmet need to provide effective treatment to prevent disease progression that is attributed in part to a lack of comprehensive understanding of asthma pathogenesis. As such, current treatment focuses on alleviating symptoms by using inhaled corticosteroids and β_2-adrenergic agonists.[3] T_H2 cells and their associated cytokines, mainly IL-4, IL-5, and IL-13, were initially identified as key players in driving the pathogenesis of allergic asthma.[4] However, recent identification of a new group of lymphocytes termed type 2 innate lymphoid cells (ILC2s) has changed the existing paradigm.

ILC2s are localized primarily at mucosal surfaces and have been found in the lung, skin, gut, and adipose tissue of both mice and human subjects.[5,6] In the lungs ILC2s drive the development of AHR and pulmonary eosinophilia triggered by allergens, such as *Alternaria alternata*, and influenza virus infection in a T cell–independent manner[7,8] and have been associated with corticosteroid-resistant asthma.[9] In addition to their role as effector cells, ILC2s are crucial in bridging the innate and adaptive responses because recent studies demonstrated that ILC2s are essential for initiation of T cell–mediated T_H2 responses.[10-12] However, unlike T cells, ILC2s lack antigen receptors and are activated rapidly by the epithelially derived cytokines IL-33, IL-25, and thymic stromal lymphopoietin and lipid mediators, including leukotriene D_4. On activation, these cells proliferate rapidly and produce high levels of the T_H2 cytokines IL-13 and IL-5.[13] The biological mechanisms that dictate ILC2 activation and proliferation and cytokine production have not been fully characterized and thus have been the subject of extensive research in recent years.

Microbial metabolites produced by the intestinal microbiota exert immunomodulatory functions that are beneficial to the host. Among these metabolites, short-chain fatty acids (SCFAs) have emerged into the limelight since the discovery of their role in driving regulatory T (Treg) cell differentiation and maintenance of homeostasis in the gut.[14,15] SCFAs consist of 2- to 5-carbon (C) weak acids, including acetate (2C), propionate (3C), and butyrate (4C), and are the end products of dietary fiber fermentation by anaerobic bacteria from the phyla Bacteroidetes and Firmicutes, among others.[16,17] Both propionate and butyrate play a protective role in intestinal inflammation through their direct influence on Treg cells.[14,15] In addition to their anti-inflammatory properties in the gut, SCFAs have been demonstrated recently to regulate allergic inflammation. For instance, propionate protected against house dust mite–driven allergic airway inflammation by impairing the ability of dendritic cells to promote T-cell effector function.[18] In another study maternal intake of acetate protected adult offspring from allergic airway diseases through epigenetic regulation of forkhead box p3 (Foxp3) in Treg cells.[19] However, the role of SCFAs in the regulation of ILC2-mediated airway inflammation remains unclear.

Here we investigated the effect of SCFAs on ILC2 function in the context of allergic airway inflammation. We found that butyrate, but not acetate or propionate, inhibits cytokine production by ILC2s at the transcription level. We demonstrate further that both systemic and local administration of butyrate attenuated ILC2-driven AHR and eosinophilic inflammation in response to *A alternata* and IL-33. Mechanistically, butyrate inhibited ILC2 proliferation and cytokine production without affecting cell viability through its histone deacetylase (HDAC) inhibitory activity and not through activation of G-coupled protein receptor (GPR) 41 or GPR43. We also show that butyrate can attenuate cytokine production by human ILC2s in humanized mice. Taken together, this study sheds new light on the immunomodulatory role of butyrate in the regulation of ILC2 function.

METHODS

Mice

BALB/c mice were purchased from the National Laboratory Animal Center (Taipei, Taiwan). Recombination-activating gene 2 $(Rag2)^{-/-}$ mice were purchased from Taconic Farms (Hudson, NY), whereas OT-II and NOD SCID (nonobese diabetic severe combined immunodeficiency) γC-deficient (NSG) mice were purchased from the Jackson Laboratory (Bar Harbor, Me). All animals were housed under specific pathogen-free conditions. Experiments were performed with sex-matched mice aged 3 to 10 weeks.

Airway allergy models and systemic administration of IL-33

Mice were challenged intranasally with 5 μg of *A alternata* (Greer Labs, Lenoir, NC) daily for 4 days. Airway inflammation was assessed 24 hours after the last challenge. In the IL-33 model mice were given 0.1 μg of recombinant murine IL-33 (BioLegend, San Diego, Calif) once daily for 3 days through the intranasal route. Airway inflammation was assessed 3 days later. Alternatively,

2 μg of IL-33 was administered intraperitoneally for 5 days, and mice were killed 24 hours later.

In vivo butyrate treatment

Mice were given drinking water containing 150 mmol/L butyrate (Sigma-Aldrich, St Louis, Mo) at pH 7.5 or saline as a control from 3 weeks of age for 6 weeks before exposure to *A alternata* or IL-33 and throughout the study. Drinking water was replaced twice a week. Alternatively, intranasal administration 10 mmol/L butyrate or saline was performed daily 2 days before exposure to *A alternata* or IL-33 and throughout the study.

Measurement of airway AHR and collection of bronchoalveolar lavage fluid

Mice were anesthetized with pentobarbital (Sigma-Aldrich) at 20 mg/kg body weight. Lung function of tracheotomized and mechanically ventilated mice was determined by means of direct measurement of airway resistance in response to increasing methacholine (Sigma-Aldrich) doses through the FinePointe RC system (Buxco Research Systems, Wilmington, NC). Bronchoalveolar lavage fluid (BALF) was collected after evaluation of lung function. For further details, see the Methods section in this article's Online Repository at www.jacionline.org.

Lung and blood sample processing for flow cytometry

Lung and blood samples were harvested and processed as described in the Methods section in this article's Online Repository.

Cell sorting and flow cytometry

Single-cell suspensions were processed for flow cytometric analysis, as described in the Methods section in this article's Online Repository. Murine ILC2s were sorted from $Rag2^{-/-}$ mice given 0.1 μg of IL-33 for 3 consecutive days and rested for 3 days to obtain sufficient numbers of lung ILC2s for sorting. Naive lung ILCs were sorted from untreated $Rag2^{-/-}$ mice. Sorting of IL-33–activated ILC2s and naive innate lymphoid cells (ILCs) was performed with a FACSAria cell sorter (BD Biosciences, Mountain View, Calif) with a sorting purity of greater than 95%.

Isolation and culture of human ILC2s

Human PBMCs were obtained from healthy human donors by using Ficoll-Paque PLUS (GE Healthcare, Uppsala, Sweden) and subjected to lineage depletion with an autoMACS column (Miltenyi Biotec, Bergisch Gladbach, Germany). Human ILC2s were sorted with a FACSAria III cell sorter (BD Biosciences). Cells were cultured in RPMI 1460 supplemented with IL-2 (50 ng/mL), IL-7 (50 ng/mL), and IL-33 (100 ng/mL).

Humanized mice

Adoptive transfer of PBMCs into NSG mice was performed, as previously described,[20] with modifications. Briefly, PBMCs were isolated from whole blood by means of separation over a Histopaque density gradient and injected intravenously into NSG mice at a density of 1×10^7 cells per mouse. Butyrate (10 mmol/L per mouse per day) was administered intranasally, whereas recombinant human IL-33, IL-2, and IL-7 (500 ng per mouse per day) were administered by means of intraperitoneal injection for 3 days. Mice were killed 24 hours later.

Statistical tests

Statistical analyses were performed with Prism 6 software (GraphPad software, La Jolla, Calif). Two-way ANOVA and the Student 2-tailed *t* test were used to determine statistical significance between groups, where *P* values of less than .05 were considered significant.

Study approval

Animal studies were approved by Academia Sinica Institutional Animal Care and Use Committee, and all experiments were performed according to the guidelines of the Institutional Animal Care and Use Committee. Informed consent was obtained from each donor as requested and approved by the Academia Sinica Institutional Review Board.

Additional information on the methods used in this study can be found in the Methods section in this article's Online Repository.

RESULTS

Butyrate inhibits cytokine production by ILC2s *in vitro*

To determine whether SCFAs can regulate ILC2 function, we first assessed the effect of acetate, propionate, and butyrate on type 2 cytokine production by IL-33–activated ILC2s. $Rag2^{-/-}$ mice were pretreated with IL-33 to facilitate ILC2 expansion, and lung ILC2s were sorted as Lin^-ST2^+ cells (see Fig E1, *A*, in this article's Online Repository at www.jacionline.org). The phenotype of these cells was confirmed further by expression of Thy1.2, inducible costimulator (ICOS), CD25, CD127, GATA3, and KLRG1 (see Fig E1, *B*). We treated sorted lung ILC2s with SCFAs in the presence of IL-33 and found that butyrate, but not acetate or propionate, markedly reduced IL-13 and IL-5 levels in the supernatant of cultured ILC2s in a dose-dependent manner (Fig 1, *A*).

To determine whether this was due to impaired cytokine production, we performed intracellular staining of IL-13 and IL-5 in ILC2s treated with SCFAs for 48 hours in the presence of IL-33. Compared with acetate and propionate, butyrate had the most potent effect in suppressing cytokine production. Although propionate slightly reduced the percentage of $IL\text{-}13^+IL\text{-}5^+$ ILC2s, the percentage of $IL\text{-}13^-IL\text{-}5^-$ ILC2s did not differ greatly. On the other hand, butyrate dose-dependently reduced the percentage of $IL\text{-}13^+IL\text{-}5^+$ ILC2s, whereas the percentage of $IL\text{-}13^-IL\text{-}5^-$ ILC2s was increased markedly (Fig 1, *B*). Accordingly, numbers of total $IL\text{-}13^+IL\text{-}5^+$ ILC2s were reduced by butyrate, but not acetate or propionate, in a dose-dependent manner (Fig 1, *C*).

Suppression was found to occur at the transcription level because quantitative real-time PCR analysis showed significant reduction in both *Il13* and *Il5* mRNA expression levels after 6 hours of treatment (Fig 1, *D*). Because these cells were pre-exposed to IL-33 *in vivo*, we next assessed whether butyrate had a similar effect on naive ILC2s activated *in vitro*. To this end, we isolated naive ILCs (sorted as $Lin^-Thy1.2^+$ cells see Fig E1, *C*; purity and CD127 expression are shown in Fig E1, *D*) from the lungs of $Rag2^{-/-}$ mice and cultured them with IL-33 in the presence or absence of butyrate. As shown in Fig 1, *E*, we found that butyrate also reduced IL-13 and IL-5 levels in the supernatants of these cells but not those of IL-17A and IFN-γ, suggesting that other ILCs were unaffected.

Systemic administration of butyrate ameliorates ILC2-mediated AHR and lung inflammation

IL-13 and IL-5 cytokines produced by ILC2s play a critical role in the development of AHR and eosinophilic inflammation.[8,10] To assess the physiologic significance of our *in vitro* data, we used *A alternata*, a clinically relevant allergen shown to activate ILC2s and trigger AHR and type 2 inflammation in mice.[21] Circulating

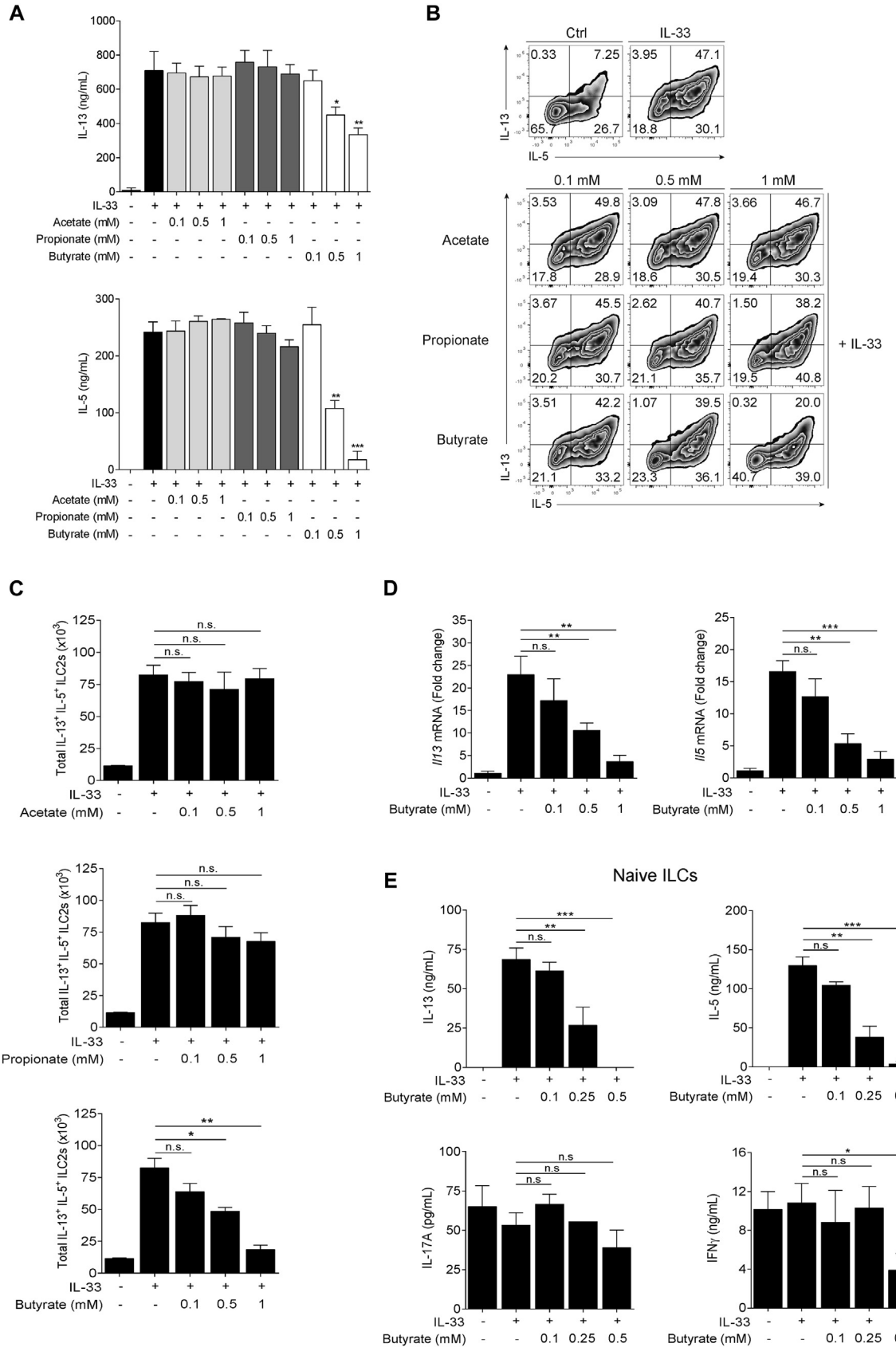
A
IL-13 (ng/mL)
IL-5 (ng/mL)
IL-33
Acetate (mM)
Propionate (mM)
Butyrate (mM)
B
Ctrl
IL-33
0.1 mM
0.5 mM
1 mM
Acetate
Propionate
Butyrate
+ IL-33
IL-13
IL-5
C
Total IL-13+ IL-5+ ILC2s (x10³)
n.s.
D
Il13 mRNA (Fold change)
Il5 mRNA (Fold change)
E
Naive ILCs
IL-13 (ng/mL)
IL-5 (ng/mL)
IL-17A (pg/mL)
IFNγ (ng/mL)

SCFAs derived from the intestinal microbiota have been shown to exert a protective effect against allergic airway inflammation.[18,22] Therefore we exposed 3-week-old mice to butyrate through drinking water to mimic circulating SCFAs for 6 weeks before intranasal *A alternata* exposure (Fig 2, *A*, protocol 1). As expected, *A alternata* administration increased lung resistance, whereas administration of butyrate without allergen challenge did not lead to increased resistance. However, butyrate-treated mice showed lower resistance than their saline-treated counterparts when challenged with *A alternata* ($P < .001$; Fig 2, *B*, solid compared with open triangles). Total eosinophil counts in the BALF of mice receiving butyrate before allergen challenge were also significantly lower than those in mice receiving saline before allergen exposure (Fig 2, *C*). Accordingly, levels of IL-13 and IL-5 in the lungs were reduced in *A alternata*–treated mice pre-exposed to butyrate compared with *A alternata*–treated mice receiving saline (Fig 2, *D*). Flow cytometry revealed that administration of butyrate before allergen challenge reduced the percentage (Fig 2, *E*) and total number (Fig 2, *F*) of lung ILC2s ($Lin^-Thy1.2^+ST2^+ICOS^+CD127^+GATA3^+$ cells). Butyrate administration also reduced total lung leukocytes induced by *A alternata* (Fig 2, *G*), and this is largely attributed to the decrease in total lung eosinophil counts but not other immune cell subsets (see Fig E2 in this article's Online Repository at www.jacionline.org).

In addition to pulmonary ILC2s, we also assessed the effect of butyrate on circulating ILC2s. Mice were treated with butyrate in drinking water for 6 weeks, followed by intraperitoneal injection of IL-33 (Fig 2, *A*, protocol 2). Flow analysis of peripheral blood leukocytes showed that butyrate also reduced the percentage (Fig 2, *H*) and total number (Fig 2, *I*) of IL-33–induced peripheral blood ILC2s. These data suggest that butyrate can inhibit both lung and circulating ILC2s.

Local administration of butyrate ameliorates ILC2-mediated AHR and lung inflammation

Although circulating SCFAs can inhibit allergic airway inflammation,[22] this effect might be due to exposure of circulatory immune cells to SCFAs rather than direct contact of SCFAs with lung immune cells, as previously suggested.[21] To rule out this possibility, we administered butyrate through the intranasal route, which allows more direct targeting of the lung mucosal immune cells.[23] Butyrate was administered daily 2 days before *A alternata* exposure and throughout the study (Fig 3, *A*). Similar to circulating butyrate, local administration of butyrate also partially suppressed AHR ($P < .001$; Fig 3, *B*, solid compared with open triangles), total BALF cell counts (Fig 3, *C*), total BALF eosinophil counts (Fig 3, *D*, and see Fig E3, *A* in this article's Online Repository at www.jacionline.org), and type 2 cytokine levels in both BALF (Fig 3, *E*) and lung tissue (Fig 3, *F*). Numbers of BALF T cells and, to a lesser extent, B cells were also reduced in percentage on butyrate exposure under inflammatory conditions (see Fig E3, *B*). Flow cytometric analysis revealed a decrease in total numbers (Fig 3, *G*) and percentages (Fig 3, *H*) of *A alternata*–induced lung ILC2s on butyrate treatment. Although we observed a slight decrease in the number of steady-state ILC2s with butyrate treatment, this is likely due to the overall decrease in numbers of total leukocytes (Fig 3, *I*), particularly eosinophils, neutrophils, and T and B cells (see Fig E3, *C* and *D*), because the population percentage did not differ between the saline- and butyrate-treated groups (Fig 3, *H*). Consistent with these findings, butyrate pretreatment ameliorated allergen-induced epithelial thickening (Fig 3, *J* and *K*), as well as IL-13–mediated mucus hypersecretion (Fig 3, *J* and *L*), as determined by using hematoxylin and eosin and periodic acid–Schiff staining, respectively.

Both colonic and lung Treg cells can be induced by SCFAs, including butyrate.[15,22] Treg cells have been demonstrated to ameliorate ILC2-mediated AHR and airway inflammation.[24] Hence, to exclude the role of Treg cells, we first examined whether butyrate administration led to Treg cell induction in the lungs. We did not observe an increase in the Treg cell population when butyrate was administered through drinking water (Fig 4, *A*). Although *A alternata* significantly increased the lung Treg cell population, butyrate treatment did not further increase percentages (Fig 4, *A*) or total numbers (Fig 4, *B*). When administered intranasally, butyrate decreased Treg cell numbers (Fig 4, *C*) but not percentages (Fig 4, *D*) at steady state, suggesting that the reduction in Treg cell numbers, as with ILC2 numbers (Fig 3, *G*), was due to an overall decrease in total lung leukocyte counts. We further assessed the ability of butyrate to suppress ILC2-mediated AHR in $Rag2^{-/-}$ mice, which lack B and T cells, including Treg cells. Similar to wild-type mice, intranasal administration of butyrate could inhibit *A alternata*–induced AHR in these knockout mice ($P < .001$; Fig 4, *E*, solid compared with open triangles). Total BALF cell (Fig 4, *F*) and BALF eosinophil (Fig 4, *G*, and see Fig E4, *A*, in this article's Online Repository at www.jacionline.org) counts were also inhibited significantly. A similar reduction in the number and percentage of eosinophils was observed in the lungs (see Fig E4, *B* and *C*). Importantly, total BALF lymphocytes, which include ILC2s, were suppressed (Fig 4, *H*). Accordingly, levels of BALF IL-13 and IL-5 were significantly lower in allergen-exposed mice receiving butyrate compared with allergen-exposed mice receiving saline (Fig 4, *I*). The observed suppression correlated with the inhibition of allergen-induced lung ILC2 expansion (Fig 4, *J*).

To further confirm the role of butyrate in suppressing ILC2-dependent AHR, we treated wild-type mice with IL-33,

FIG 1. Butyrate, but not acetate or propionate, inhibits cytokine production in ILC2s. ILC2s (Fig 1, *A-D*) were sorted from the lungs of IL-33–treated $Rag2^{-/-}$ mice, whereas total ILCs (Fig 1, *E*) were sorted from naive $Rag2^{-/-}$ mice. Cells were treated with 10 ng/mL (Fig 1, *A-D*) or 50 ng/mL (Fig 1, *E*) IL-33 in the absence or presence of acetate, propionate, or butyrate at the indicated concentrations. **A,** IL-13 and IL-5 levels in culture supernatants of ILC2s treated for 48 hours. **B,** Representative flow diagram showing intracellular expression of IL-13 and IL-5 in ILC2s after 48 hours of treatment. **C,** Total $IL\text{-}13^+IL\text{-}5^+$ ILC2s after 48 hours of treatment assessed as in Fig 1, *B*. **D,** *Il13* and *Il5* mRNA expression after 6 hours of treatment. **E,** IL-13, IL-5, IL-17A, and IFN-γ levels in culture supernatants of ILCs treated for 5 days. All cultures contained IL-2 and IL-7 (both at 10 ng/mL). Data are shown as means ± SDs from 1 of 3 independent experiments (n = 3 wells) with consistent findings. *n.s.*, Not significant. $*P < .05$, $**P < .01$, and $***P < .001$ (compared with the IL-33–treated group).

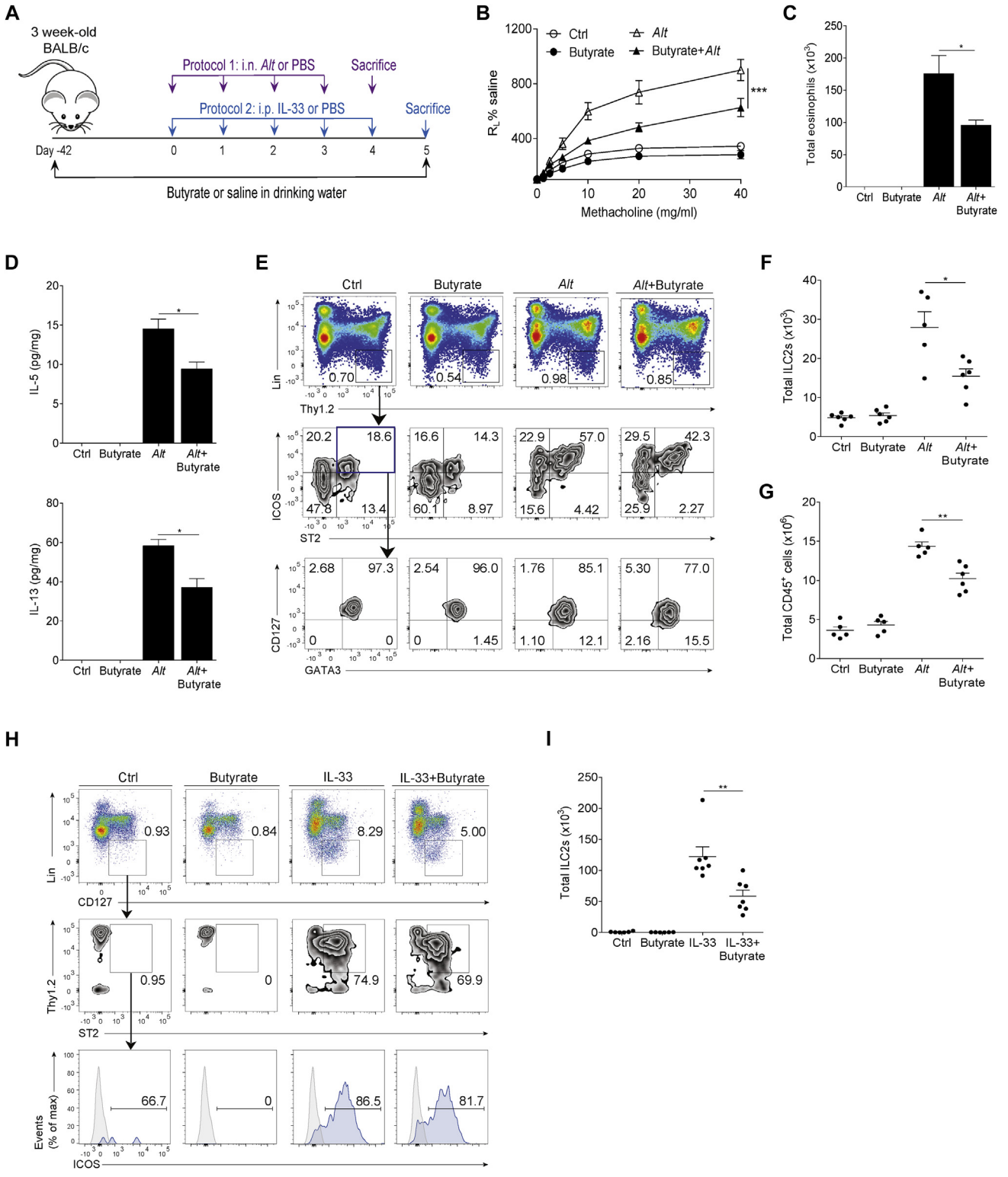

FIG 2. Administration of butyrate in drinking water ameliorates ILC2-dependent airway inflammation. **A,** Schematic diagram of butyrate treatment in drinking water of BALB/c mice exposed to *A alternata* (protocol 1; Fig 2, *B-G*) or IL-33 (protocol 2; Fig 2, *H* and *I*) through the intranasal *(i.n.)* and intraperitoneal *(i.p.)* routes, respectively. **B,** Lung resistance in response to increasing doses of methacholine. **C,** Total eosinophils in BALF. **D,** IL-5 and IL-13 levels in lung homogenates of mice. **E,** Representative flow diagram showing the lung ILC2 population ($Lin^-Thy1.2^+ST2^+ICOS^+CD127^+GATA3^+$) gated from viable $CD45^+$ cells. **F,** Total number of lung ILC2s per mouse assessed as in Fig 2, *E*. **G,** Total number of $CD45^+$ cells in the lungs per mouse gated from viable cells. **H,** Representative flow diagram showing ILC2 population ($Lin^-CD127^+Thy1.2^+ST2^+ICOS^+$) in blood gated from viable $CD45^+$ cells. Representative histograms are shown, whereby *gray solid lines* indicate isotype-matched control and *blue solid lines* indicate antibody staining. **I,** Total number of ILC2s in blood per mouse assessed as in Fig 2, *H*. Data are shown as means ± SEMs of 2 independent experiments (n = 5-7 each). $*P < .05$, $**P < .01$, and $***P < .0001$.

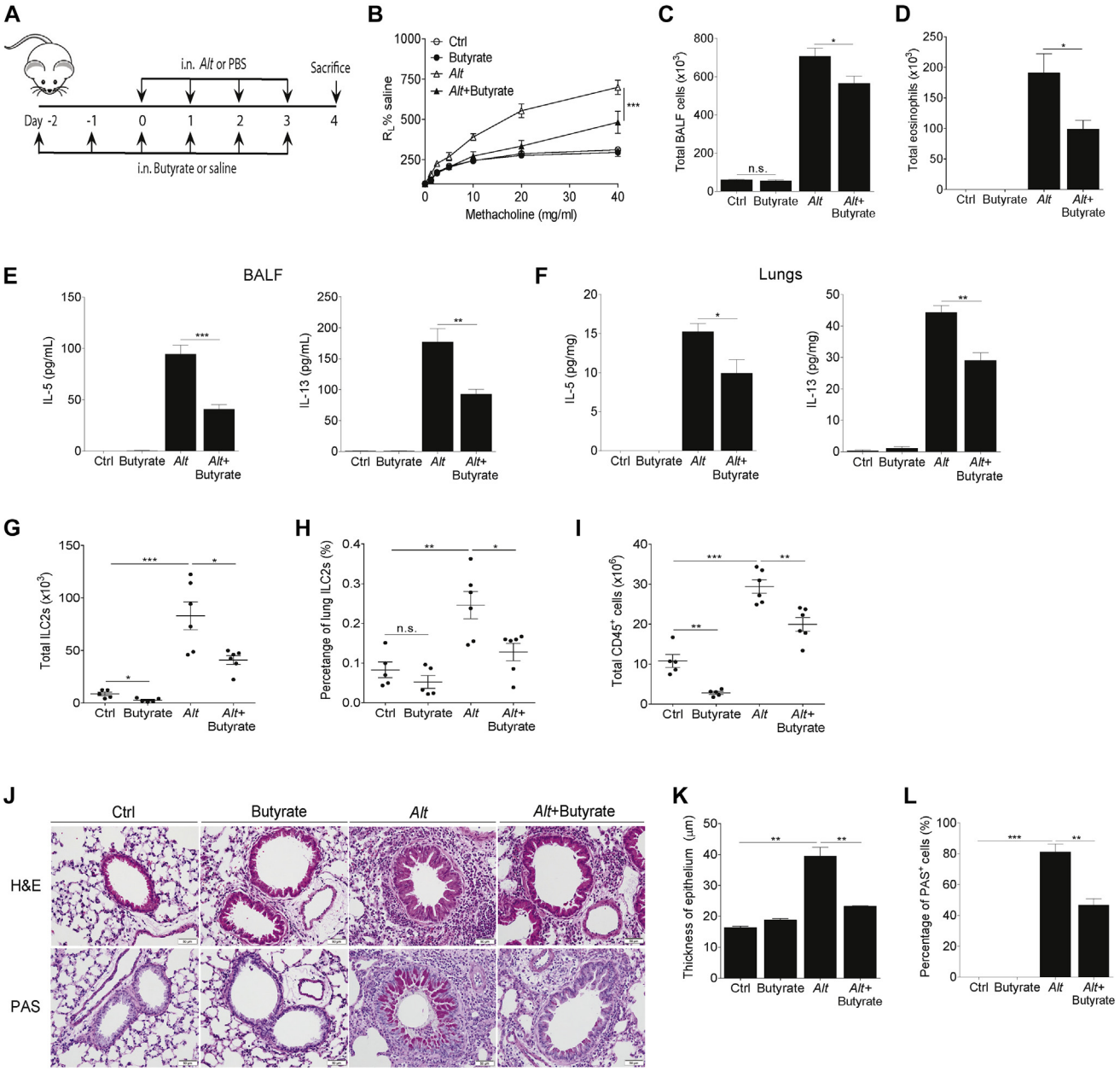

FIG 3. Intranasal administration of butyrate prevents ILC2-mediated airway inflammation. **A,** Schematic diagram of butyrate treatment by means of intranasal *(i.n.)* delivery in an *A alternata* model of airway inflammation in BALB/c mice. **B,** Lung resistance in response to increasing doses of methacholine. **C** and **D,** Total cells (Fig 3, *C*) and eosinophils (Fig 3, *D*) in BALF. **E** and **F,** IL-5 and IL-13 levels in BALF (Fig 3, *E*) and lung homogenates (Fig 3, *F*) of mice. **G** and **H,** Total number (Fig 3, *G*) and percentage (Fig 3, *H*) of lung ILC2s per mouse. **I,** Total number of $CD45^+$ cells in the lungs per mouse. **J,** Representative images of hematoxylin and eosin *(H&E)*– and periodic acid–Schiff *(PAS)*–stained histologic sections of the lungs of mice. *Scale bars* = 50 μm. **K,** Quantification of epithelial thickness (in micrometers). **L,** Percentage of PAS^+ cells in airway epithelium. Data are shown as means ± SEMs of 2 independent experiments (n = 5-6 each). $*P < .05$, $**P < .01$, and $***P < .0001$.

an epithelially derived cytokine that specifically activates ILC2s and causes AHR.[25] To this end, we treated the mice daily with butyrate administered through the intranasal route 2 days before IL-33 administration and throughout the study (see Fig E5, *A*, in this article's Online Repository at www.jacionline.org). As with the allergen model, pre-exposure to butyrate significantly but partially inhibited IL-33–induced AHR ($P < .01$; see Fig E5, *B*, solid circles compared with solid triangles), as well as total BALF cell counts (see Fig E5, *C*), BALF eosinophil counts (see Fig E5, *D*), and levels of lung IL-5 and IL-13 (see Fig E5, *E*), which corresponded to the reduction in total ILC2 numbers (see Fig E5, *F*). Overall, these data confirm that butyrate plays an inhibitory role in ILC2-mediated AHR and lung inflammation.

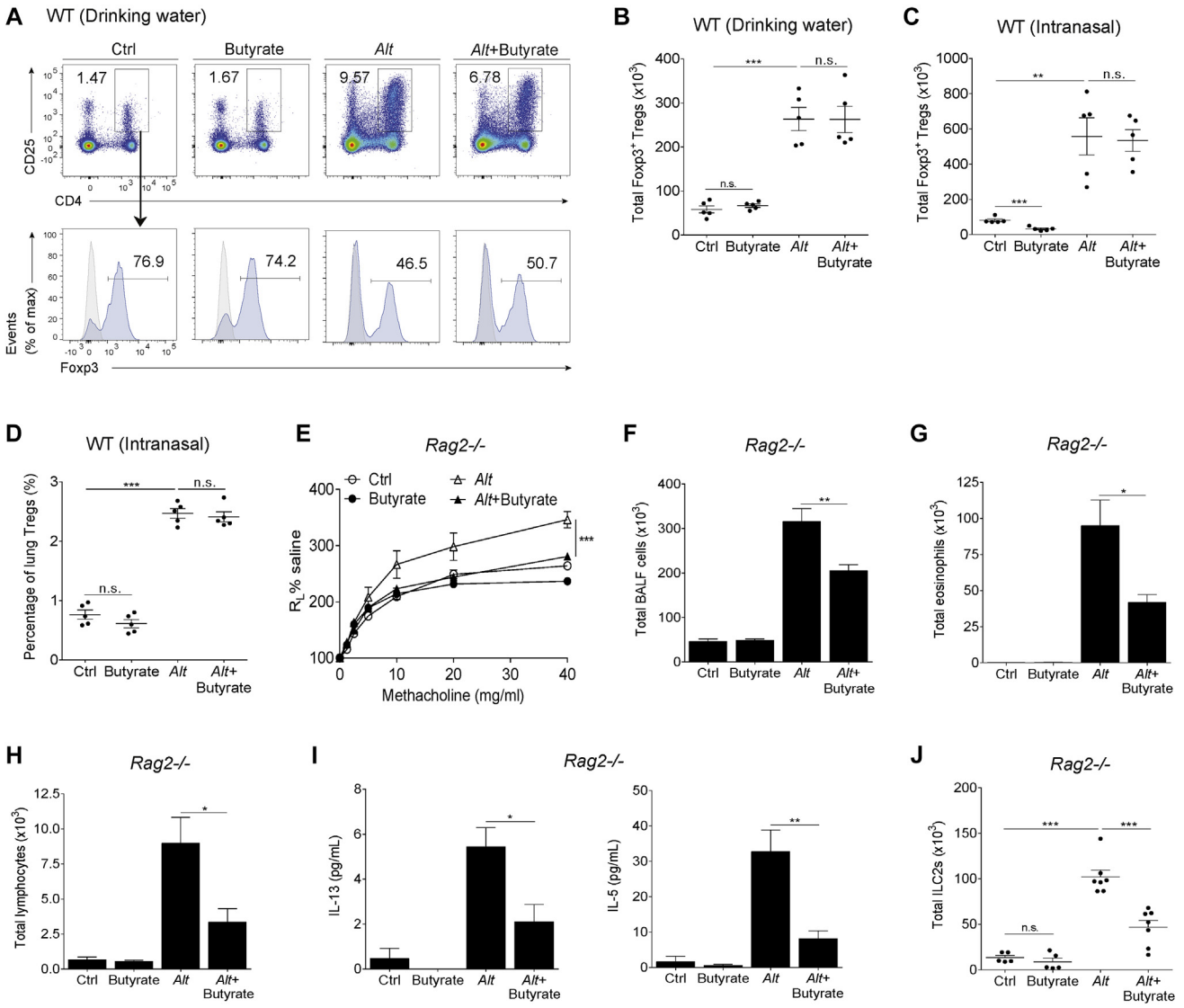

FIG 4. Butyrate-mediated suppression occurs independently of adaptive immunity. BALB/c wild-type *(WT)* or *Rag2*$^{-/-}$ mice received PBS or *A alternata* with or without butyrate treatment through drinking water (Fig 4, *A* and *B*; according to protocol 1 in Fig 2, *A*) or the intranasal route (Fig 4, *C-J*; according to the protocol in Fig 3, *A*). **A,** Representative flow diagram showing the lung Treg cell population ($CD4^+CD25^+Foxp3^+$) gated from viable $CD45^+$ cells in BALB/c mice. Representative histograms are shown, whereby *gray solid lines* indicate isotype-matched control and *blue solid lines* indicate antibody staining. **B** and **C,** Total Treg cells in lungs of BALB/c mice treated with butyrate through drinking water (Fig 4, *B*) or the intranasal route (Fig 4, *C*) assessed as in Fig 4, *A*. **D,** Percentage of Treg cells in the lungs of BALB/c mice receiving butyrate intranasally. **E,** Lung resistance of *Rag2*$^{-/-}$ mice in response to increasing doses of methacholine. **F-H,** Total cells (Fig 4, *F*), eosinophils (Fig 4, *G*), and lymphocytes (Fig 4, *H*) in the BALF of *Rag2*$^{-/-}$ mice. **I,** IL-5 and IL-13 levels in the BALF of *Rag2*$^{-/-}$ mice. **J,** Total number of lung ILC2s per *Rag2*$^{-/-}$ mouse. Data are shown as means ± SEMs of 3 independent experiments (n = 5-7 each). *n.s.*, Not significant. **P* < .05, ***P* < .01, and ****P* < .0001.

Butyrate attenuates ILC2 proliferation and GATA3 expression

Butyrate has been shown to inhibit proliferation and induce apoptosis in various immune and nonimmune cell types.[26,27] To evaluate whether butyrate exerts similar effect on ILC2s, we sorted lung ILC2s and cultured them with IL-33 in the absence or presence of butyrate. Analysis of cell viability by using fixable viability dye (FVD) staining revealed that butyrate did not induce significant cell death at a concentration of 1 mmol/L or less (Fig 5, *A*). Because FVD staining does not differentiate between apoptotic and nonapoptotic cells, we further stained ILC2s with Annexin V/propidium iodide (PI) and found that the percentages of cells undergoing early apoptosis (Annexin V^+PI^- cells) and late apoptosis/necrosis (Annexin V^+PI^+ cells)[28] increased only slightly (<5% at 1 mmol/L) in a dose-dependent manner (Fig 5, *B*) and is therefore unlikely to have caused the marked decrease in mRNA and protein levels of IL-13 and IL-5 (Fig 1, *A* and *D*).

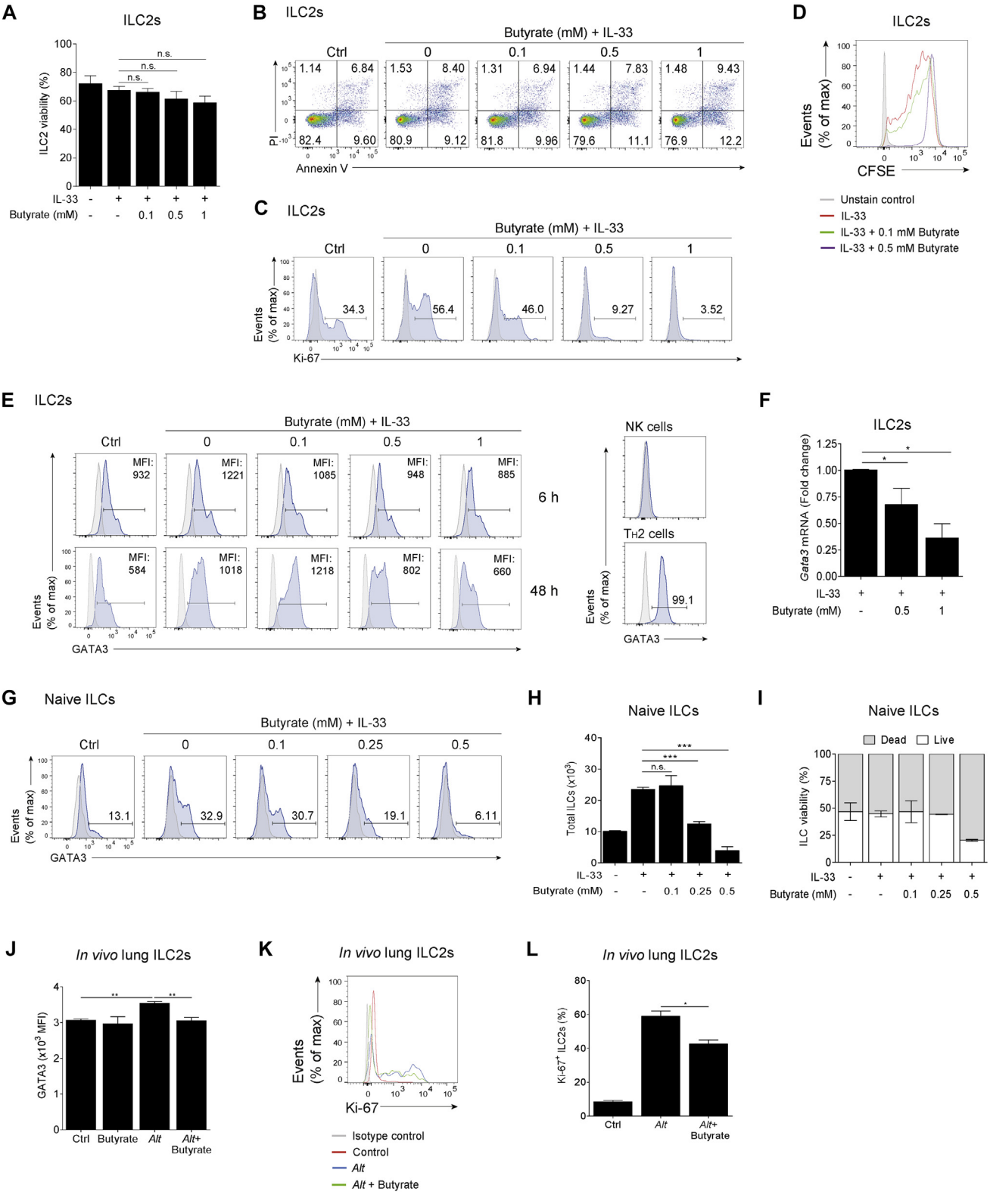
A
ILC2s
ILC2 viability (%)
n.s.
IL-33
Butyrate (mM)
B
ILC2s
Butyrate (mM) + IL-33
Ctrl
PI
Annexin V
C
ILC2s
Ki-67
Events (% of max)
D
ILC2s
CFSE
Unstain control
IL-33
IL-33 + 0.1 mM Butyrate
IL-33 + 0.5 mM Butyrate
E
ILC2s
GATA3
6 h
48 h
NK cells
TH2 cells
F
ILC2s
Gata3 mRNA (Fold change)
G
Naive ILCs
H
Naive ILCs
Total ILCs (x10³)
I
Naive ILCs
Dead
Live
ILC viability (%)
J
In vivo lung ILC2s
GATA3 (x10³ MFI)
Ctrl
Butyrate
Alt
Alt+ Butyrate
K
In vivo lung ILC2s
Isotype control
Control
Alt
Alt + Butyrate
L
In vivo lung ILC2s
Ki-67⁺ ILC2s (%)

We then assessed the proliferation rate of ILC2s by using Ki-67 and carboxyfluorescein succinimidyl ester (CFSE) staining. As expected, IL-33 treatment increased the proliferation capacity of ILC2s when compared with unstimulated control cells, as indicated by the increase in the percentage of Ki-67$^+$ cells (Fig 5, *C*). Butyrate treatment markedly decreased the percentage of Ki-67$^+$ ILC2s, causing near-complete inhibition at a dose of 0.5 mmol/L. The inhibition was sustained for up to 5 days, as determined by using CFSE staining (Fig 5, *D*).

We next assessed the effect of butyrate on the expression of GATA3 in ILC2s activated with IL-33 and treated with butyrate *in vitro*. Butyrate treatment reduced GATA3 expression in terms of mean fluorescence intensity as early as 6 hours after treatment in a dose-dependent manner (Fig 5, *E*, and see Fig E6, *A* and *B*, in this article's Online Repository at www.jacionline.org). A minimum dose of 0.5 mmol/L was required for the inhibition, which corresponded to the dose required to inhibit cytokine production at the mRNA and protein levels (Fig 1, *A* and *D*). Likewise, the expression of *Gata3* mRNA was significantly reduced by butyrate treatment (Fig 5, *F*). Butyrate also inhibited the expansion of IL-33–induced GATA3$^+$ ILC2s from the pool of naive ILC culture at a minimum concentration of 0.25 mmol/L (Fig 5, *G*, and see Fig E6, *C*). Inhibition of proliferation was also observed at this dose, as evident by the reduction in total ILC numbers (Fig 5, *H*), although this was not attributed to cell death (Fig 5, *I*).

We further confirmed these findings *in vivo* by using the allergen model. ILC2s were exposed to butyrate through intranasal delivery and challenged with *A alternata*, as in Fig 3, *A*. Similar to our *in vitro* findings, butyrate can ameliorate GATA3 induction by *A alternata* (Fig 5, *J*, and see Fig E6, *D*). Under steady-state conditions, a majority of lung ILC2s were negative for Ki-67 staining. Allergen challenge significantly increased the Ki-67$^+$ population, with a fraction of ILC2s expressing high levels of Ki-67 (Fig 5, *K*). Importantly, butyrate treatment reduced this population, as well as the overall percentage of Ki-67$^+$ ILC2s (Fig 5, *L*).

Butyrate does not affect pathways downstream of IL-33/ST2 signaling

To investigate the mechanism by which butyrate exerts its inhibitory function, we first evaluated the activation state of several proteins downstream of IL-33/ST2 signaling. Multiplex bead array analysis on the phosphorylation state of 4 kinases (p38, Akt, extracellular signal-regulated kinase [ERK], and c-Jun N-terminal kinase) downstream of the ST2 receptor revealed no significant difference between butyrate-treated and untreated ILC2s activated with IL-33 (see Fig E7, *A-D*, in this article's Online Repository at www.jacionline.org). Additionally, IL-33 induced nuclear factor κB (NF-κB) phosphorylation to the same extent in the presence or absence of butyrate (see Fig E7, *E*). These data suggest that butyrate does not affect IL-33/ST2 signaling pathways.

GPR41 activation does not affect ILC2 function

SCFAs have been shown to activate GPR41 (FFAR3) and GPR43 (FFAR2), although butyrate preferentially activates GPR41.[29,30] We assessed the expression of GPR41 in ILC2s and found that IL-33 treatment significantly upregulated mRNA levels of GPR41 when compared with control values, and butyrate cotreatment did not affect expression levels (Fig 6, *A*). To determine the role of GPR41 activation on ILC2 function, we treated IL-33–activated ILC2s with the GPR41 agonist AR420626 and measured cytokine levels in the supernatant. Unlike butyrate, AR420626 treatment did not attenuate the levels of IL-33–induced IL-13 and IL-5 (Fig 6, *B*). Furthermore, flow cytometric analysis of Ki-67 revealed no significant differences between untreated and AR420626-treated ILC2s, suggesting that the agonist does not impair ILC2 proliferation (Fig 6, *C*). Likewise, expression of GATA3, which was induced by IL-33, was not affected by AR420626 treatment (Fig 6, *D*). In addition, AR420626 treatment did not affect the ability of butyrate to inhibit IL-13 and IL-5 production by ILC2s (Fig 6, *E*). Overall, these results imply that GPR41 activation does not affect ILC2 function or proliferation and that the inhibitory effect of butyrate is likely to be GPR41 independent.

We also evaluated the effect of GPR43 activation on ILC2 function. Similar to GPR41, IL-33 upregulated the mRNA level of GPR43, although this was inhibited by butyrate (see Fig E8, *A*, in this article's Online Repository at www.jacionline.org). We found that 4-CMTB, a GPR43 agonist, increased ILC2 cell proliferation in a dose-dependent manner (see Fig E8, *B*) but had no effect on GATA3 expression (see Fig E8, *C*). Interestingly, however, IL-13 and IL-5 levels in the supernatant were reduced by 4-CMTB treatment (see Fig E8, *D*). More importantly, butyrate cotreatment with 4-CMTB resulted in synergistic inhibition, suggesting that butyrate does not go through the GPR43-mediated pathway.

FIG 5. Butyrate inhibits ILC2 proliferation and GATA3 expression but not viability. ILC2s were sorted from the lungs of IL-33–treated *Rag2*$^{-/-}$ mice (Fig 5, *A-F*), whereas total ILCs were sorted from naive *Rag2*$^{-/-}$ mice (Fig 5, *G-I*). Cells were cultured with 10 ng/mL (Fig 5, *A-F*) or 50 ng/mL (Fig 5, *G-I*) IL-33, IL-2, and IL-7 (both at 10 ng/mL) in the presence or absence of butyrate at the indicated concentrations. Control cells were cultured with IL-2 and IL-7 only (both at 10 ng/mL). **A,** Percentage of viable ILC2s after 48 hours of treatment, as determined by using FVD staining. **B,** Representative flow diagram showing PI$^+$ and Annexin V$^+$ ILC2s after 48 hours of treatment. **C** and **D,** Proliferation of ILC2s, as assessed by using Ki-67 (Fig 5, *C*) and CFSE staining (Fig 5, *D*) after 48 hours and 5 days of treatment, respectively. **E,** Mean fluorescence intensity *(MFI)* of GATA3 in ILC2s after 6 or 48 hours of treatment. GATA3 expression of natural killer *(NK)* cells and T cells are shown as controls. **F,** *Gata3* mRNA expression after 6 hours of treatment. **G,** Percentage of GATA3$^+$ ILCs after 5 days of treatment. **H** and **I,** Total number (Fig 5, *H*) and percentage viability (Fig 5, *I*) of ILCs after 5 days of treatment. Data are shown as means ± SDs from 1 of 2 independent experiments (n = 3 wells) with consistent findings. Representative histograms are shown, whereby *gray solid lines* indicate isotype-matched control and *blue solid lines* indicate antibody staining. **J-L,** BALB/c mice were treated with butyrate and *A alternata* intranasally, as in Fig 3, *A*. Fig 5, *J*, MFI of GATA3. Fig 5, *K* and *L*, Representative flow diagram of Ki-67 (Fig 5, *K*) and percentage Ki-67$^+$ lung ILC2s (Fig 5, *L*). Data are shown as means ± SEMs from 2 independent experiments (n = 4-5 each). *n.s.*, Not significant. **P* < .05, ***P* < .01, and ****P* < .001.

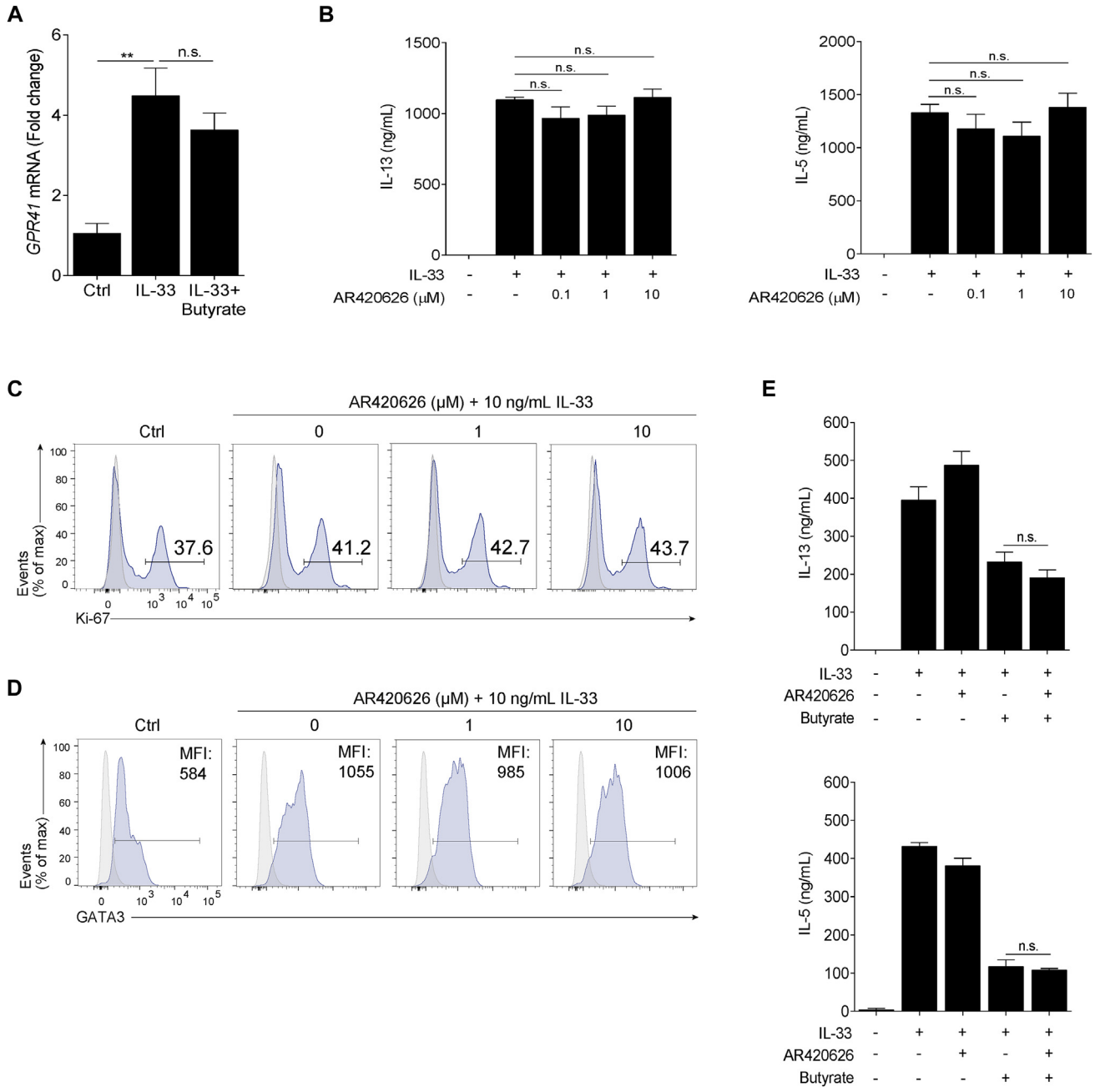

FIG 6. GPR41 agonist does not impair ILC2 proliferation and function. ILC2s were sorted from the lungs of IL-33–treated *Rag2*$^{-/-}$ mice and cultured with IL-33, IL-2, and IL-7 (all at 10 ng/mL) in the presence or absence of butyrate, AR420626, or both at the indicated concentrations. Control cells were cultured with IL-2 and IL-7 only (both at 10 ng/mL). **A,** *GPR41* mRNA expression after 6 hours of treatment with IL-33 in the presence or absence of 1 mmol/L butyrate. **B,** IL-13 and IL-5 levels in culture supernatants of ILC2s after 48 hours of treatment. **C,** Proliferation of ILC2s, as assessed by using Ki-67 after 48 hours of treatment. **D,** Representative flow diagram showing GATA3 expression in ILC2s after treatment for 48 hours. Representative histograms are shown, whereby *gray solid lines* indicate isotype-matched control and *blue solid lines* indicate antibody staining. *MFI*, Mean fluorescence intensity. **E,** IL-13 and IL-5 levels in culture supernatants of ILC2s after 48 hours of treatment with 1 μmol/L AR420626, 0.5 mmol/L butyrate, or both in the presence of IL-33 (10 ng/mL). Data are shown as means ± SDs from 1 of 3 independent experiments (n = 3 wells) with consistent findings. *n.s.*, Not significant. ***P* < .01.

Butyrate exerts its inhibitory effects through HDAC inhibition

Aside from activation of GPRs, SCFAs also exhibit HDAC inhibitory activity and can induce histone acetylation in multiple cell types.[31-33] To determine whether butyrate acts as an HDAC inhibitor in ILC2s, we analyzed the levels of H3 acetylation and HDAC activity in comparison with trichostatin A (TSA), a well-established HDAC inhibitor. Although IL-33 has been

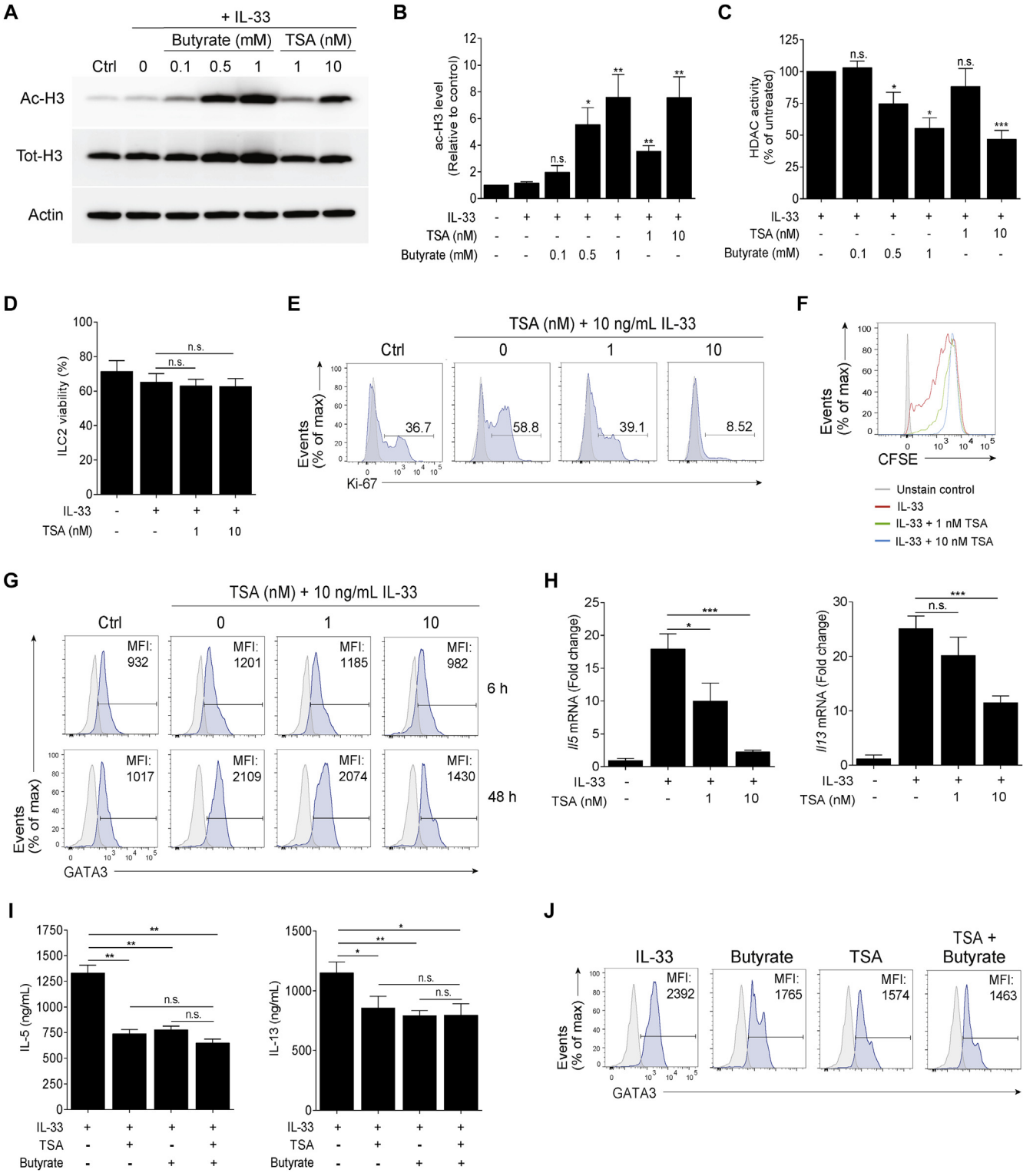

FIG 7. Butyrate-mediated suppression of ILC2 function occurs through its HDAC inhibitory activity. ILC2s sorted from the lungs of IL-33–treated *Rag2*$^{-/-}$ mice were cultured with IL-33, IL-2, and IL-7 (all at 10 ng/mL) with or without butyrate, TSA, or both at the indicated concentrations. Control cells were cultured with IL-2 and IL-7 only (both at 10 ng/mL). **A** and **B,** Representative western blot image (Fig 7, *A*) and relative expression (Fig 7, *B*) of ac-H3 level after 6 hours of treatment. Data were normalized against total H3. **C,** HDAC activity in ILC2 nuclear extracts after 6 hours of treatment. **D,** Percentage of viable ILC2s after 48 hours of treatment, as determined by using FVD staining. **E** and **F,** Proliferation of ILC2s, as assessed by using Ki-67 (Fig 7, *E*) and CFSE staining (Fig 7, *F*) after 48 hours and 5 days of treatment, respectively. **G,** Mean fluorescence intensity *(MFI)* of GATA3 in ILC2s after treatment for 6 and 48 hours. **H,** *Il13* and *Il5* mRNA expression after 6 hours treatment. **I** and **J,** Sorted lung ILC2s were treated with 10 nmol/L TSA, 0.5 mmol/L butyrate, or both in the presence of IL-33 (10 ng/mL) for 48 hours. Fig 7, *I*, IL-13 and IL-5 levels in culture supernatants of ILC2s. Fig 7, *J*, MFI of GATA3. Representative histograms are shown, whereby *gray solid lines* indicate isotype-matched control and *blue solid lines* indicate antibody staining. Data are shown as means ± SDs from 1 of 2 to 3 independent experiments (n = 3 wells) with consistent findings. *n.s.*, Not significant. **P* < .05, ***P* < .01, and ****P* < .001.

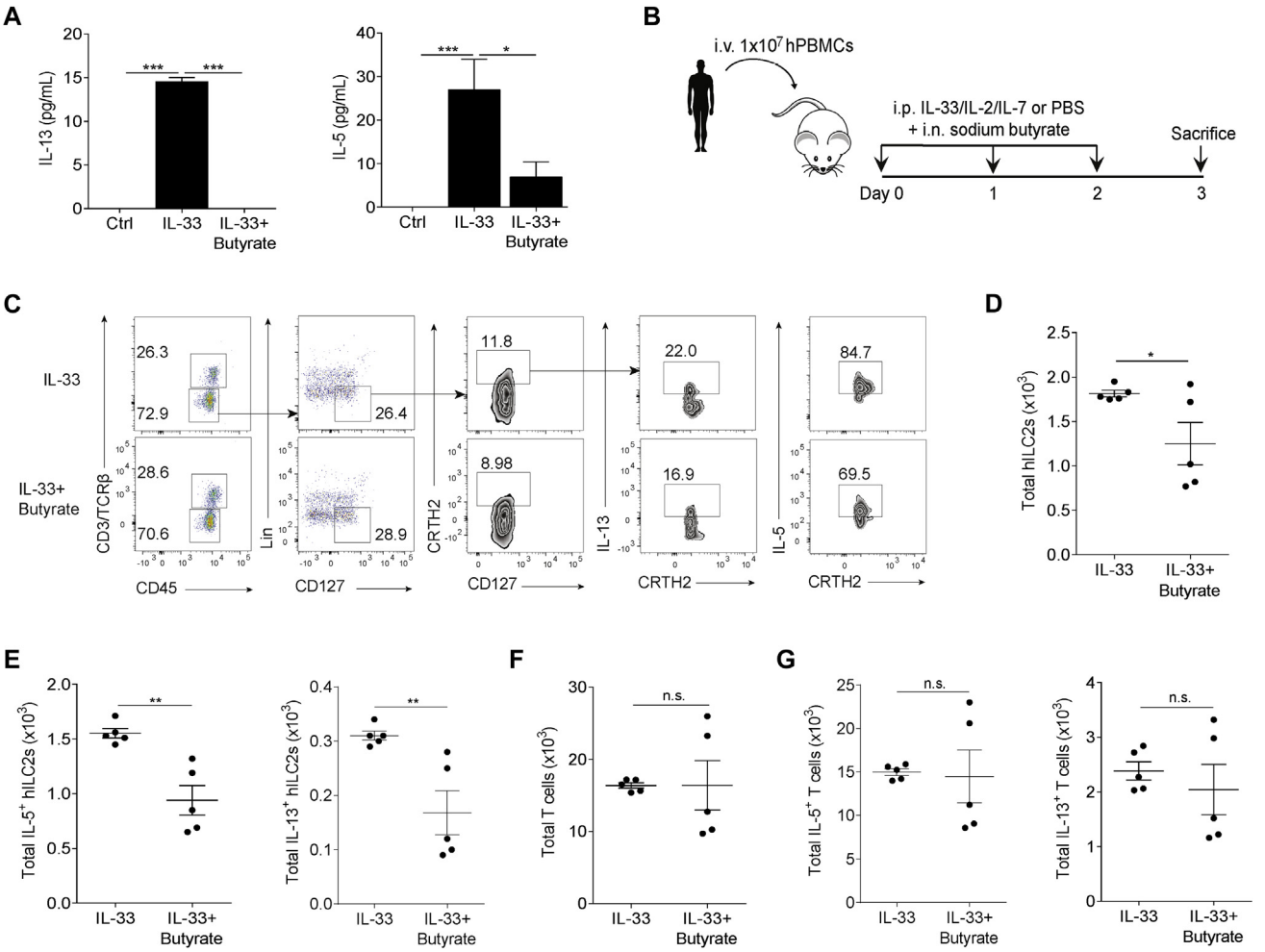

FIG 8. Butyrate inhibits cytokine production by IL-33–activated human ILC2s. Human ILC2s were sorted from healthy donor PBMCs and cultured with IL-33 (100 ng/mL), IL-2 (10 ng/mL), and IL-7 (10 ng/mL) in the presence or absence of butyrate at the indicated concentrations. **A,** IL-13 and IL-5 levels in culture supernatants of human ILC2s after 3 days of treatment. Data are shown as means ± SDs from 1 of 2 independent experiments (n = 3 wells) with consistent findings. **B,** Schematic diagram showing IL-33 and butyrate treatment in NSG mice after adoptive transfer of PBMCs from healthy donors. *i.n.*, Intranasal; *i.p.*, intraperitoneal; *i.v.*, intravenous. **C,** Representative flow diagram showing intracellular expression of IL-13 and IL-5 in human ILC2s ($CD45^+Lin^-CD127^+CRTH2^+$) isolated from the lungs of NSG mice. **D,** Total human ILC2s in the lung per mouse. **E,** Total $IL\text{-}13^+$ and $IL\text{-}5^+$ ILC2s in the lung per mouse. **F,** Total human T cells ($CD45^+CD3/TCR\beta^+$) in the lung per mouse. **G,** Total $IL\text{-}13^+$ and $IL\text{-}5^+$ T cells in the lung per mouse. Data are shown as means ± SEMs from 2 independent experiments (n = 5). *n.s.*, Not significant. $^*P < .05$, $^{**}P < .01$, and $^{***}P < .001$.

shown to induce histone acetylation in some cell types, such as mast cells,[34] no notable increment in total H3 acetylation was observed in ILC2s treated with the same stimulus. However, both butyrate and TSA treatment significantly augmented the levels of H3 acetylation (Fig 7, *A* and *B*), whereas HDAC activity was reduced in a dose-dependent manner (Fig 7, *C*). We also tested the H3 acetylation effect of acetate and propionate and found that although acetate did not alter the level of H3 acetylation, propionate weakly induced H3 acetylation when compared with butyrate (see Fig E9 in this article's Online Repository at www.jacionline.org).

To investigate the importance of HDAC inhibition in ILC2 function, we treated IL-33–activated ILC2s with increasing concentrations of TSA and evaluated its effect on ILC2 viability, proliferation, and cytokine production. Although TSA treatment at a concentration as high as 10 nmol/L did not affect cell viability (Fig 7, *D*), ILC2 proliferation was significantly impaired, as shown by Ki-67 (Fig 7, *E*) and CFSE staining (Fig 7, *F*). Similar to butyrate, GATA3 expression (Fig 7, *G*, and see Fig E10, *A*, in this article's Online Repository at www.jacionline.org), as well as *Il13* and *Il5* mRNA levels (Fig 7, *H*), were significantly ameliorated by TSA treatment in a dose-dependent manner, suggesting that HDAC inhibition impaired ILC2 proliferation and function.

To determine whether butyrate-mediated inhibition is dependent on its HDAC inhibitory activity, we cotreated ILC2s with butyrate and TSA in the presence of IL-33. Butyrate has been shown to act on similar HDAC targets as TSA in dendritic cells through cotreatment strategy.[35] Like butyrate, we found that TSA can also inhibit IL-13 and IL-5 production at the protein level. Interestingly, cotreatment of TSA and butyrate did not exhibit any synergistic or additive effects (Fig 7, *I*). Accordingly, butyrate

treatment did not further enhance TSA-mediated GATA3 inhibition (Fig 7, *J*, and see Fig E10, *B*). These data support the hypothesis that butyrate inhibits ILC2 function through inhibition of HDAC activity.

Butyrate inhibits cytokine production by human ILC2s

To assess the effect of butyrate in human ILC2s, we sorted these cells from PBMCs of healthy donors and cultured them in IL-33 in the absence or presence of butyrate for 3 days. Levels of IL-13 and IL-5 in culture supernatants were measured by means of ELISA. Similar to murine ILC2s, butyrate potently inhibited IL-13 and IL-5 production in human ILC2s (Fig 8, *A*). We confirmed these data by using humanized PBMCs from mice treated with IL-33 with or without pre-exposure to butyrate through the intranasal route (Fig 8, *B*). ILC2s were gated as the $CD45^+Lin^-CD127^+CRTH2^+$ population after exclusion of T cells ($CD45^+$CD3/T-cell receptor [TCR] β^+; Fig 8, *C*). We found that butyrate treatment reduced the percentage (Fig 8, *C*, third column) and total number (Fig 8, *D*) of ILC2s. Importantly, intracellular staining of type 2 cytokines revealed a significant reduction in the percentage (Fig 8, *C*, fourth and fifth column) and total number (Fig 8, *E*) of IL-13– and IL-5–producing ILC2s. Notably, butyrate did not alter the percentage (Fig 8, *C*, first column) or total number (Fig 8, *F*) of $CD3^+$ T cells, nor did it affect the overall frequency of IL-13– and IL-5–producing T cells (Fig 8, *G*). Collectively, these data suggest that butyrate exerts similar inhibitory effects on human ILC2s.

DISCUSSION

Recent evidence has implicated gut microbial metabolites in the regulation of allergic airway inflammation in the context of adaptive immunity.[14,15] Although adaptive immunity holds a pivotal role in orchestrating the cardinal features of asthma, ILC2s take central stage in driving acute asthma exacerbations triggered by allergens, such as *A alternata*.[36] However, the role of microbial metabolites in the regulation of ILC2-driven allergic inflammation has yet to be elucidated. For the first time, we show that the microbial metabolite butyrate directly regulates ILC2 function and attenuates ILC2-mediated AHR and airway inflammation.

SCFAs, such as acetate, propionate, and butyrate, have been shown to promote Treg cell generation in separate studies.[14,35] Additionally, SCFAs promote naive T-cell differentiation into T_H1 and T_H17 effector cells,[37] whereas their roles in T_H2 responses have been shown to be inhibitory and are mediated through interaction with other immune cells.[18,22] Here we show that only butyrate inhibited IL-13 and IL-5 production by murine ILC2s. Because high concentrations of butyrate (>1 mmol/L) have been shown to induce cell apoptosis,[38,39] we further excluded cell death as a possibility for the observed suppression by showing that butyrate treatment (up to 1 mmol/L concentration) did not augment the percentage of apoptotic cells. Importantly, we demonstrate that butyrate can inhibit type 2 cytokine production by human ILC2s transferred into NSG mice.

Recent evidence suggests an inverse correlation between a high-fiber diet and asthma severity in patients.[40] This is supported by the finding that a high-fiber diet increased circulating SCFAs and provided protection against allergic airway disease in mice.[18] Similarly, butyrate administered through drinking water suppressed the cardinal features of allergen-induced inflammation, including AHR, eosinophil infiltration, and T_H2 cytokine release, through inhibition of lung ILC2 expansion. We also show that short-term intranasal administration of butyrate can ameliorate both *A alternata*–induced AHR and airway inflammation to a similar degree as circulating butyrate. The lung microbiome has been implicated in the orchestration of the outcome of allergic disorders. For instance, SCFA-producing phyla, including Bacteroidetes, Firmicutes, and Fusobacteria, have been identified in the respiratory tracts of healthy subjects and asthmatic patients, and a strong correlation exists between the severity of asthma and microbial dysbiosis in the lungs.[41,42] Moreover, a recent study showed that bacteria isolated from the lungs can produce SCFAs, although correlation between SCFA production and asthma development remains controversial.[43] Hence our study provides supporting evidence that local production of metabolites can influence the outcome of airway allergy.

The total SCFAs in gut lumen is approximately 100 to 150 mmol/L, whereas the concentration of SCFAs in the bloodstream is vastly lower at 0.1 to 1 mmol/L under normal physiologic conditions.[44-46] This is due to the large uptake of SCFAs by colonic epithelial cells (>95%), with only a small proportion being absorbed into the portal circulation.[45,47] To mimic the physiologic condition, we fed mice with 150 mmol/L butyrate (drinking water), a concentration previously used by others.[14,48] Meanwhile, the concentration of lung SCFAs in healthy subjects is not well defined, although it can reach up to 2 mmol/L in the sputum of patients with cystic fibrosis.[49] Nevertheless, intranasal administration of butyrate at 10 mg/mL (approximately 1 mol/L) has been shown to protect against allergic rhinitis.[50] However, because of concerns with toxicity, we resorted to a lower dose (10 mmol/L). We found that both treatment regimens partially but significantly reduced the ILC2 population and airway inflammation. Because butyrate acted in a dose-dependent manner *in vitro*, we reasoned that the partial inhibition might be due to the amount of butyrate reaching lung ILC2s, given that it is likely to be taken up by other immune and nonimmune cells either through passive diffusion or GPRs present on other cells, such as bronchial epithelial cells, dendritic cells, and neutrophils.[18,51,52]

We also observed that butyrate treatment administered through the intranasal route, but not through drinking water, reduced T- and B-cell populations in the lungs at both steady state and during allergen-induced inflammation. This might be due to differences in bioavailability and pharmacokinetic properties between the 2 modes of administration,[53] as well as the final concentration and duration of butyrate exposure in the lungs. Extensive studies will be required to dissect the underlying mechanism of inhibition in these cells, although some studies have shown that butyrate can induce apoptosis in T cells and modulate B-cell differentiation.[54,55] Nevertheless, the effects of butyrate on both lymphocyte populations do not contribute to its suppressive effect in ILC2s, as demonstrated in our $Rag2^{-/-}$ mouse model.

A recent study found that SCFA production by *Heligmosomoides polygyrus* significantly augments house dust mite–induced lung IL-10 and TGF-β levels and Treg cell suppressor function, although the lung Treg cell proportion was only slightly increased.[22] In this study, however, we did not observe any changes in lung Treg cell

numbers after butyrate exposure either through drinking water or the intranasal route. Moreover, no significant increase in levels of lung IL-10 and TGF-β was observed through either method of butyrate administration under allergen-induced inflammatory conditions (data not shown). Importantly, butyrate inhibited ILC2s in the absence of Treg cells, as demonstrated in *Rag2*$^{-/-}$ mice. Therefore, although we do not completely rule out the possibility that butyrate can affect Treg cell function, Treg cells are not required for the inhibitory effects of butyrate on ILC2s in the *A alternata* model.

We found that butyrate reduced numbers of murine ILC2s in the lungs after IL-33 and *A alternata* treatment. Likewise, IL-33–induced human ILC2 expansion was attenuated by butyrate treatment in NSG mice. It has been shown previously that *A alternata* induces ILC2 accumulation in an IL-33–dependent manner.[8] IL-33 promotes local ILC2 proliferation and expansion in the lungs rather than recruitment from other tissues.[56] This led us to hypothesize that butyrate can affect ILC2 proliferation. In support of this, butyrate is known to inhibit proliferation in multiple cell types.[26,27] Consistent with our hypothesis, we found that butyrate inhibits murine ILC2 proliferation both *in vitro* and *in vivo*. In addition, we found that inhibition of IL-13 and IL-5 expression occurred at the transcription level. Because GATA3 is the master regulator for transcription of the *Il13* and *Il5* genes,[57] we assessed the effect of butyrate on GATA3 expression *in vitro*. Similar to a previous study,[58] we found that IL-33 could induce GATA3 expression in cultured ILC2s. Although a previous study demonstrated that butyrate does not affect GATA3 expression in T cells,[15] we found that GATA3 expression was attenuated on butyrate exposure at both the protein and mRNA levels. This suppression likely led to impaired cytokine production and attenuated ILC2-induced AHR and lung inflammation.

The anti-inflammatory role of butyrate has been attributed to multiple factors, including inhibition of NF-κB activation in various immune cell types,[59] although a recent study showed that butyrate does not affect NF-κB or mitogen-activated protein kinase signaling pathways downstream of Toll-like receptor 4 in LPS-stimulated macrophages.[60] Similar to this study, we found that butyrate does not affect signaling downstream of the ST2 receptor. We also show that butyrate does not act through either GPR41 or GPR43, both of which are induced by IL-33 at the mRNA level. This is based on the observation that the GPR41 agonist did not affect ILC2 function, whereas the GPR43 agonist and butyrate treatment led to synergistic inhibition of cytokine secretion. Moreover, GPRs have been shown to activate ERK and p38 mitogen-activated protein kinase signaling pathways.[61] However, our bead array data show that butyrate treatment did not induce any increase in ERK and p38 phosphorylation, affirming that butyrate-mediated suppression is independent of GPR activation. Because SCFAs can be readily absorbed into any cell types through simple diffusion or active transportation through soluble transporters,[62,63] it is likely that butyrate is taken up by ILC2s through either of these mechanisms, thus bypassing the GPR receptors, although more extensive studies will be required to elucidate the pathway involved.

It is widely known that butyrate acts as an HDAC inhibitor in many cell types. In this study we show that both butyrate and TSA, a pan-HDAC inhibitor, augment the level of acetylated H3 at lysines 9 and 14 and inhibit HDAC activity. TSA has been reported to suppress ILC2-mediated allergic inflammation in mice by reducing the number of lung ILC2s.[64] In agreement with this finding, we show that TSA phenocopies the effect of butyrate in terms of attenuating T_H2 cytokine production, GATA3 expression, and proliferation. Importantly, we show that TSA and butyrate cotreatment did not result in synergistic effects, further suggesting that butyrate acts as an HDAC inhibitor in ILC2s. Histone acetylation leads to transcriptional activation because of DNA unwinding, which increases access of basal transcription factors and RNA polymerase II to the promoter region.[65] However, this modification has also been shown to recruit chromatin-repressive complexes, such as Mi-2/NURD, and cause transcriptional inhibition in macrophages.[66] Whether the inhibitory effect of butyrate/TSA is due to direct acetylation of T_H2-related genes or indirectly through transcriptional activation/repression of other targets that can alter the expression of T_H2-related genes warrants further investigation.

HDAC inhibitory activity is not limited to butyrate because other SCFAs, such as propionate and acetate, also exhibit such activity, although to a varying degree of potency. Acetate is known to be a weak HDAC inhibitor,[31] whereas the inhibitory activity of propionate has been reported to be lower than butyrate.[67] Indeed, acetate has been shown to exhibit little to no effect on H3 acetylation in dendritic cells, whereas propionate induced H3 acetylation to a lower degree than butyrate.[35] In line with these findings, we observed that acetate did not induce H3 acetylation at 1 mmol/L, whereas H3 acetylation by propionate at a concentration of 1 mmol/L was significantly lower than that caused by butyrate. This likely explains the lack of inhibition by acetate and the slight suppression of IL-5 by propionate at 1 mmol/L in IL-33–stimulated cultured ILC2s (Fig 1, *A* and *B*). In the case of propionate, a higher concentration might be required to achieve a more prominent suppression.

In conclusion, we demonstrate that both local and systemic administration of butyrate inhibit ILC2 proliferation and cytokine production likely through inhibition of GATA3 expression. As a consequence, allergic airway inflammation is attenuated. Mechanistically, we prove that butyrate acts through inhibition of HDACs in a GPR-independent manner. Our work highlights the importance of butyrate as an immunomodulatory metabolite in controlling allergic inflammation. Given that *A alternata* and ILC2s have been associated with corticosteroid-resistant asthma,[68,69] this finding might be of potential clinical relevance and might open up new therapeutic avenues for the treatment of corticosteroid-resistant asthma.

We thank the staff of the IBMS Flow Cytometry Core Facility for services and facilities provided.

Key messages

- **Butyrate directly inhibits ILC2 proliferation and cytokine function through GATA3 inhibition without affecting cell survival.**
- **Butyrate acts through HDAC inhibition and H3 acetylation independent of GPR41 and GPR43.**
- **Inhibition of ILC2 function by butyrate ameliorates *A alternata* and IL-33–mediated AHR and airway inflammation.**
- **Similar inhibition was observed in human ILC2s both *in vivo* and *in vitro*.**

REFERENCES

1. Possa SS, Leick EA, Prado CM, Martins MA, Tiberio IF. Eosinophilic inflammation in allergic asthma. Front Pharmacol 2013;4:46.
2. Walsh ER, Stokes K, August A. The role of eosinophils in allergic airway inflammation. Discov Med 2010;9:357-62.
3. Tamm M, Richards DH, Beghe B, Fabbri L. Inhaled corticosteroid and long-acting beta2-agonist pharmacological profiles: effective asthma therapy in practice. Respir Med 2012;106(suppl 1):S9-19.
4. Lambrecht BN, Hammad H. The immunology of asthma. Nat Immunol 2015;16:45-56.
5. Drake LY, Kita H. Group 2 innate lymphoid cells in the lung. Adv Immunol 2014;124:1-16.
6. Brestoff JR, Kim BS, Saenz SA, Stine RR, Monticelli LA, Sonnenberg GF, et al. Group 2 innate lymphoid cells promote beiging of white adipose tissue and limit obesity. Nature 2015;519:242-6.
7. Chang YJ, Kim HY, Albacker LA, Baumgarth N, McKenzie AN, Smith DE, et al. Innate lymphoid cells mediate influenza-induced airway hyper-reactivity independently of adaptive immunity. Nat Immunol 2011;12:631-8.
8. Bartemes KR, Iijima K, Kobayashi T, Kephart GM, McKenzie AN, Kita H. IL-33-responsive lineage- CD25+ CD44(hi) lymphoid cells mediate innate type 2 immunity and allergic inflammation in the lungs. J Immunol 2012;188:1503-13.
9. Liu S, Verma M, Michalec L, Liu W, Sripada A, Rollins D, et al. Steroid resistance of airway type 2 innate lymphoid cells from patients with severe asthma: the role of thymic stromal lymphopoietin. J Allergy Clin Immunol 2018;141:257-68.e6.
10. Halim TY, Steer CA, Matha L, Gold MJ, Martinez-Gonzalez I, McNagny KM, et al. Group 2 innate lymphoid cells are critical for the initiation of adaptive T helper 2 cell-mediated allergic lung inflammation. Immunity 2014;40:425-35.
11. Barlow JL, Bellosi A, Hardman CS, Drynan LF, Wong SH, Cruickshank JP, et al. Innate IL-13-producing nuocytes arise during allergic lung inflammation and contribute to airways hyperreactivity. J Allergy Clin Immunol 2012;129:191-8, e1-4.
12. Halim TY, Hwang YY, Scanlon ST, Zaghouani H, Garbi N, Fallon PG, et al. Group 2 innate lymphoid cells license dendritic cells to potentiate memory TH2 cell responses. Nat Immunol 2016;17:57-64.
13. Lund S, Walford HH, Doherty TA. Type 2 innate lymphoid cells in allergic disease. Curr Immunol Rev 2013;9:214-21.
14. Smith PM, Howitt MR, Panikov N, Michaud M, Gallini CA, Bohlooly YM, et al. The microbial metabolites, short-chain fatty acids, regulate colonic Treg cell homeostasis. Science 2013;341:569-73.
15. Furusawa Y, Obata Y, Fukuda S, Endo TA, Nakato G, Takahashi D, et al. Commensal microbe-derived butyrate induces the differentiation of colonic regulatory T cells. Nature 2013;504:446-50.
16. den Besten G, van Eunen K, Groen AK, Venema K, Reijngoud DJ, Bakker BM. The role of short-chain fatty acids in the interplay between diet, gut microbiota, and host energy metabolism. J Lipid Res 2013;54:2325-40.
17. Canani RB, Costanzo MD, Leone L, Pedata M, Meli R, Calignano A. Potential beneficial effects of butyrate in intestinal and extraintestinal diseases. World J Gastroenterol 2011;17:1519-28.
18. Trompette A, Gollwitzer ES, Yadava K, Sichelstiel AK, Sprenger N, Ngom-Bru C, et al. Gut microbiota metabolism of dietary fiber influences allergic airway disease and hematopoiesis. Nat Med 2014;20:159-66.
19. Thorburn AN, McKenzie CI, Shen S, Stanley D, Macia L, Mason LJ, et al. Evidence that asthma is a developmental origin disease influenced by maternal diet and bacterial metabolites. Nat Commun 2015;6:7320.
20. Taylor S, Huang Y, Mallett G, Stathopoulou C, Felizardo TC, Sun MA, et al. PD-1 regulates KLRG1+ group 2 innate lymphoid cells. J Exp Med 2017;214:1663-78.
21. Doherty TA, Khorram N, Chang JE, Kim HK, Rosenthal P, Croft M, et al. STAT6 regulates natural helper cell proliferation during lung inflammation initiated by *Alternaria*. Am J Physiol Lung Cell Mol Physiol 2012;303:L577-88.
22. Zaiss MM, Rapin A, Lebon L, Dubey LK, Mosconi I, Sarter K, et al. The intestinal microbiota contributes to the ability of helminths to modulate allergic inflammation. Immunity 2015;43:998-1010.
23. Derrick SC, Kolibab K, Yang A, Morris SL. Intranasal administration of *Mycobacterium bovis* BCG induces superior protection against aerosol infection with Mycobacterium tuberculosis in mice. Clin Vaccine Immunol 2014;21:1443-51.
24. Rigas D, Lewis G, Aron JL, Wang B, Banie H, Sankaranarayanan I, et al. Type 2 innate lymphoid cell suppression by regulatory T cells attenuates airway hyperreactivity and requires inducible T-cell costimulator-inducible T-cell costimulator ligand interaction. J Allergy Clin Immunol 2017;139:1468-77.e2.
25. Kim HY, Chang YJ, Subramanian S, Lee HH, Albacker LA, Matangkasombut P, et al. Innate lymphoid cells responding to IL-33 mediate airway hyperreactivity independently of adaptive immunity. J Allergy Clin Immunol 2012;129:216-27, e1-6.
26. Bailon E, Cueto-Sola M, Utrilla P, Rodriguez-Cabezas ME, Garrido-Mesa N, Zarzuelo A, et al. Butyrate in vitro immune-modulatory effects might be mediated through a proliferation-related induction of apoptosis. Immunobiology 2010;215:863-73.
27. Xie C, Wu B, Chen B, Shi Q, Guo J, Fan Z, et al. Histone deacetylase inhibitor sodium butyrate suppresses proliferation and promotes apoptosis in osteosarcoma cells by regulation of the MDM2-p53 signaling. Onco Targets Ther 2016;9:4005-13.
28. Suzuki J, Denning DP, Imanishi E, Horvitz HR, Nagata S. Xk-related protein 8 and CED-8 promote phosphatidylserine exposure in apoptotic cells. Science 2013;341:403-6.
29. Tazoe H, Otomo Y, Kaji I, Tanaka R, Karaki SI, Kuwahara A. Roles of short-chain fatty acids receptors, GPR41 and GPR43 on colonic functions. J Physiol Pharmacol 2008;59(suppl 2):251-62.
30. Lu Y, Fan C, Li P, Chang X, Qi K. Short chain fatty acids prevent high-fat-diet-induced obesity in mice by regulating G protein-coupled receptors and gut microbiota. Sci Rep 2016;6:37589.
31. Davie JR. Inhibition of histone deacetylase activity by butyrate. J Nutr 2003;133:2485S-93S.
32. Nguyen NH, Morland C, Gonzalez SV, Rise F, Storm-Mathisen J, Gundersen V, et al. Propionate increases neuronal histone acetylation, but is metabolized oxidatively by glia. Relevance for propionic acidemia. J Neurochem 2007;101:806-14.
33. Gao X, Lin SH, Ren F, Li JT, Chen JJ, Yao CB, et al. Acetate functions as an epigenetic metabolite to promote lipid synthesis under hypoxia. Nat Commun 2016;7:11960.
34. Ito T, Egusa C, Maeda T, Numata T, Nakano N, Nishiyama C, et al. IL-33 promotes MHC class II expression in murine mast cells. Immun Inflamm Dis 2015;3:196-208.
35. Arpaia N, Campbell C, Fan X, Dikiy S, van der Veeken J, deRoos P, et al. Metabolites produced by commensal bacteria promote peripheral regulatory T-cell generation. Nature 2013;504:451-5.
36. Kabata H, Moro K, Koyasu S, Asano K. Group 2 innate lymphoid cells and asthma. Allergol Int 2015;64:227-34.
37. Park J, Kim M, Kang SG, Jannasch AH, Cooper B, Patterson J, et al. Short-chain fatty acids induce both effector and regulatory T cells by suppression of histone deacetylases and regulation of the mTOR-S6K pathway. Mucosal Immunol 2015;8:80-93.
38. Ramos MG, Rabelo FL, Duarte T, Gazzinelli RT, Alvarez-Leite JI. Butyrate induces apoptosis in murine macrophages via caspase-3, but independent of autocrine synthesis of tumor necrosis factor and nitric oxide. Braz J Med Biol Res 2002;35:161-73.
39. Zhang J, Yi M, Zha L, Chen S, Li Z, Li C, et al. Sodium butyrate induces endoplasmic reticulum stress and autophagy in colorectal cells: implications for apoptosis. PLoS One 2016;11:e0147218.
40. Halnes I, Baines KJ, Berthon BS, MacDonald-Wicks LK, Gibson PG, Wood LG. Soluble fibre meal challenge reduces airway inflammation and expression of GPR43 and GPR41 in asthma. Nutrients 2017;9.
41. Huang YJ, Nariya S, Harris JM, Lynch SV, Choy DF, Arron JR, et al. The airway microbiome in patients with severe asthma: associations with disease features and severity. J Allergy Clin Immunol 2015;136:874-84.
42. Zhang Q, Cox M, Liang Z, Brinkmann F, Cardenas PA, Duff R, et al. Airway microbiota in severe asthma and relationship to asthma severity and phenotypes. PLoS One 2016;11:e0152724.
43. Remot A, Descamps D, Noordine ML, Boukadiri A, Mathieu E, Robert V, et al. Bacteria isolated from lung modulate asthma susceptibility in mice. ISME J 2017;11:1061-74.
44. Kiefer J, Beyer-Sehlmeyer G, Pool-Zobel BL. Mixtures of SCFA, composed according to physiologically available concentrations in the gut lumen, modulate histone acetylation in human HT29 colon cancer cells. Br J Nutr 2006;96:803-10.
45. Cummings JH, Pomare EW, Branch WJ, Naylor CP, Macfarlane GT. Short chain fatty acids in human large intestine, portal, hepatic and venous blood. Gut 1987;28:1221-7.
46. Mackie RI, White BA, Isaacson RE. Gastrointestinal Microbiology. New York: Chapman & Hall; 1997.
47. Topping DL, Clifton PM. Short-chain fatty acids and human colonic function: roles of resistant starch and nonstarch polysaccharides. Physiol Rev 2001;81:1031-64.
48. Ji J, Shu D, Zheng M, Wang J, Luo C, Wang Y, et al. Microbial metabolite butyrate facilitates M2 macrophage polarization and function. Sci Rep 2016;6:24838.

49. Ghorbani P, Santhakumar P, Hu Q, Djiadeu P, Wolever TM, Palaniyar N, et al. Short-chain fatty acids affect cystic fibrosis airway inflammation and bacterial growth. Eur Respir J 2015;46:1033-45.
50. Wang J, Wen L, Wang Y, Chen F. Therapeutic effect of histone deacetylase inhibitor, sodium butyrate, on allergic rhinitis in vivo. DNA Cell Biol 2016;35:203-8.
51. Mirkovic B, Murray MA, Lavelle GM, Molloy K, Azim AA, Gunaratnam C, et al. The role of short-chain fatty acids, produced by anaerobic bacteria, in the cystic fibrosis airway. Am J Respir Crit Care Med 2015;192:1314-24.
52. Vinolo MA, Ferguson GJ, Kulkarni S, Damoulakis G, Anderson K, Bohlooly YM, et al. SCFAs induce mouse neutrophil chemotaxis through the GPR43 receptor. PLoS One 2011;6:e21205.
53. Bardal S, Waechter J, Martin D. Chapter 2—Pharmacokinetics. In: Dimock E, Hyde M, Cicalese B, editors. Applied Pharmacology. Philadelphia: Saunders; 2011. pp. 17-34.
54. Zimmerman MA, Singh N, Martin PM, Thangaraju M, Ganapathy V, Waller JL, et al. Butyrate suppresses colonic inflammation through HDAC1-dependent Fas upregulation and Fas-mediated apoptosis of T cells. Am J Physiol Gastrointest Liver Physiol 2012;302:G1405-15.
55. Sanchez HN, Shen T, Zan H, Casali P. Short-chain fatty acid HDAC inhibitor-mediated downregulation of AID expression and class switch DNA recombination is relieved by estrogen through modulation of selected microRNAs. J Immunol 2016;196(suppl):127.
56. Martinez-Gonzalez I, Matha L, Steer CA, Ghaedi M, Poon GF, Takei F. Allergen-experienced group 2 innate lymphoid cells acquire memory-like properties and enhance allergic lung inflammation. Immunity 2016;45:198-208.
57. Yagi R, Zhong C, Northrup DL, Yu F, Bouladoux N, Spencer S, et al. The transcription factor GATA3 is critical for the development of all IL-7Ralpha-expressing innate lymphoid cells. Immunity 2014;40:378-88.
58. Furusawa J, Moro K, Motomura Y, Okamoto K, Zhu J, Takayanagi H, et al. Critical role of p38 and GATA3 in natural helper cell function. J Immunol 2013;191:1818-26.
59. Luhrs H, Gerke T, Muller JG, Melcher R, Schauber J, Boxberge F, et al. Butyrate inhibits NF-kappaB activation in lamina propria macrophages of patients with ulcerative colitis. Scand J Gastroenterol 2002;37:458-66.
60. Chang PV, Hao L, Offermanns S, Medzhitov R. The microbial metabolite butyrate regulates intestinal macrophage function via histone deacetylase inhibition. Proc Natl Acad Sci U S A 2014;111:2247-52.
61. Kim MH, Kang SG, Park JH, Yanagisawa M, Kim CH. Short-chain fatty acids activate GPR41 and GPR43 on intestinal epithelial cells to promote inflammatory responses in mice. Gastroenterology 2013;145:396-406, e1-10.
62. Hadjiagapiou C, Schmidt L, Dudeja PK, Layden TJ, Ramaswamy K. Mechanism(s) of butyrate transport in Caco-2 cells: role of monocarboxylate transporter 1. Am J Physiol Gastrointest Liver Physiol 2000;279:G775-80.
63. Kamp F, Hamilton JA. How fatty acids of different chain length enter and leave cells by free diffusion. Prostaglandins Leukot Essent Fatty Acids 2006;75:149-59.
64. Toki S, Goleniewska K, Reiss S, Zhou W, Newcomb DC, Bloodworth MH, et al. The histone deacetylase inhibitor trichostatin A suppresses murine innate allergic inflammation by blocking group 2 innate lymphoid cell (ILC2) activation. Thorax 2016;71:633-45.
65. Ito K, Adcock IM. Histone acetylation and histone deacetylation. Mol Biotechnol 2002;20:99-106.
66. Roger T, Lugrin J, Le Roy D, Goy G, Mombelli M, Koessler T, et al. Histone deacetylase inhibitors impair innate immune responses to Toll-like receptor agonists and to infection. Blood 2011;117:1205-17.
67. Rumberger JM, Arch JR, Green A. Butyrate and other short-chain fatty acids increase the rate of lipolysis in 3T3-L1 adipocytes. PeerJ 2014;2:e611.
68. Kabata H, Moro K, Fukunaga K, Suzuki Y, Miyata J, Masaki K, et al. Thymic stromal lymphopoietin induces corticosteroid resistance in natural helper cells during airway inflammation. Nat Commun 2013;4:2675.
69. Castanhinha S, Sherburn R, Walker S, Gupta A, Bossley CJ, Buckley J, et al. Pediatric severe asthma with fungal sensitization is mediated by steroid-resistant IL-33. J Allergy Clin Immunol 2015;136:312-22.e7.

METHODS

Measurement of airway AHR and collection of BALF

Mice were anesthetized with pentobarbital (Sigma-Aldrich) at 20 mg/kg body weight. Lung function of tracheotomized and mechanically ventilated mice was determined by means of direct measurement of airway resistance in response to increasing methacholine (Sigma-Aldrich) doses by using the FinePointe RC system (Buxco Research Systems). Immediately after AHR, lungs were lavaged twice with 1 mL of PBS supplemented with 2% FBS (HyClone, Logan, Utah). BALF was pooled and pelleted by means of centrifugation and fixed onto cytospin slides. Slides were stained with Diff-Quik solution (Polysciences, Warrington, Pa), and BALF differential cell counting was performed.

Antibodies, cytokines, and reagents

All antibodies were obtained from BioLegend, unless specified otherwise. The following antibodies were used for flow cytometric staining of murine samples at 1:400 dilution, unless specified otherwise: CD3ε (145-2C11), FcεRI (MAR-1), CD49b (DX5), CD11c (N418), CD11b (M1/70), F4/80 (BM8), CD19 (6D5), Ly6G (1A8; 1:200), CD103 (2E7; 1:200 dilution), NKp46 (29A1.4; 1:200 dilution), ST2 (DIH9; 1:200 dilution), CD45 (30-F11), ICOS (c398.4A; 1:200 dilution), CD25 (PC61.5; 1:200 dilution), CD127 (A7R34; 1:100 dilution), KLRG1 (2F1; 1:200), CD4 (GK1.5; 1:200 dilution), and GATA3 (16E10A23; 1:20 dilution). Thy1.2 (53-2.1), T-bet (eBio4B10; 1:50 dilution), retinoic acid–related orphan receptor γt (AFKJS-9; 1:50 dilution), Foxp3 (FJK-16s; 1:50 dilution), IL-13 (eBio13A; 1:50 dilution), and IL-5 (TRFK5; 1:50 dilution) were purchased from eBioscience (San Diego, Calif). Phospho–NF-κB p65 (Ser536; 93H1; 1:50 dilution) was purchased from CST (Danvers, Mass), whereas Siglec-F (E50-2440; 1:200 dilution) and MHC class II I-A/I-E (M5/114.15.2; 1:200 dilution) were purchased from BD Biosciences. Human ILC2s were stained with the following antibodies at 1:20 dilution, unless specified otherwise: human lineage cocktail (CD3, CD14, CD16, CD19, CD20, and CD56), FcεRI (CRA1), CD3 (HIT3a), TCRβ (IP26), CD45 (HI30), CRTH2 (BM16), CD161 (HP-3G10), IL-7 receptor α (A019D5), IL13 (JES10-5A2), and IL-5 (TRFK5; 1:50 dilution; eBioscience). Fluorochrome-conjugated FVD and Ki-67 were purchased from eBioscience. Mouse (anti-CD16/32) and human TruStain FcX (Fc blocking solution) were purchased from BioLegend. Recombinant mouse IL-33, IL-2, and IL-4 were purchased from BioLegend, whereas recombinant mouse IL-7 was obtained from PeproTech (Rocky Hill, NJ). Recombinant human IL-33 and IL-7 were purchased from BioLegend, whereas IL-2 was purchased from eBioscience. Anti-mouse IFN-γ (XMG1.2) and IL-12/IL-23 p40 (C17.8) were purchased from BioXcell (West Lebanon, NH). Phorbol 12-myristate 13-acetate (PMA) and ionomycin were obtained from Sigma-Aldrich. Brefeldin A, the Annexin V Apoptosis Detection kit, and the BD Cytofix/Cytoperm kit were purchased from BD Biosciences. The Foxp3 Transcription Factor Staining kit was purchased from eBioscience. CFSE was purchased from Cayman Chemical (Ann Arbor, Mich).

Lung and blood sample processing for flow cytometry

Whole lungs were minced and incubated in Dulbecco modified Eagle medium with 0.1% (vol/vol) DNase I (Worthington Biochemicals, Lakewood, NJ) and 1.6 mg/mL collagenase IV (Worthington Biochemicals) for 40 minutes at 37°C. Tissues were filtered through a 70-μm mesh to obtain single-cell suspensions. Red blood cells were removed from the cell suspensions by using ACK lysing buffer (Gibco Laboratories, Grand Island, NY). Single-cell suspensions were resuspended in the appropriate buffer for further processing.

Peripheral blood was collected by means of cardiac puncture in a tube containing 20 mmol/L Na_2 EDTA (Millipore, Billerica, Mass) as an anticoagulant. Mononuclear cells were isolated with Histopaque-1077 (Sigma-Aldrich) and resuspended in the appropriate buffer for further processing.

Cell sorting and flow cytometry

For surface staining, single-cell suspensions were first stained with FVD, followed by Fc blocking with anti-mouse CD16/32 or anti-human TruStain FcX, and then stained with the appropriate antibodies. Intracellular staining was performed, as previously described, with modifications.[E1] Single-cell suspensions from the lungs of mice were stimulated with 100 ng/mL PMA, 1 μg/mL ionomycin, and 1 μg/mL Brefeldin A in DMEM for 6 hours. Alternatively, PMA, ionomycin, and Brefeldin A were added directly to cultured ILC2s during the last 6 hours of culture. After surface staining, cells were fixed and permeabilized with BD Cytofix/Cytoperm solution and further stained intracellularly with anti-mouse or anti-human IL-13 and IL-5. For transcription factor staining, the Foxp3 staining buffer set was used according to the manufacturer's instructions. For detection of apoptotic cells, cells were stained with the Annexin V Apoptosis Detection kit, according to the manufacturer's recommendations. After staining, cells were washed and resuspended in FACS buffer and analyzed by using flow cytometry. Data were acquired on an LSR II (BD Biosciences) and analyzed with FlowJo v.10.1 software (TreeStar, Ashland, Ore).

Murine ILC2s were sorted from *Rag2*$^{-/-}$ mice given 0.1 μg of IL-33 for 3 consecutive days and rested for 3 days to obtain sufficient number of lung ILC2s for sorting. Naive lung ILCs were sorted from untreated *Rag2*$^{-/-}$ mice. IL-33–activated ILC2s and naive ILCs were sorted as CD45$^+$Lin$^-$ST2$^+$ and CD45$^+$Lin$^-$Thy1.2$^+$ cells, respectively. Lineage markers used are CD3, CD19, TCRβ, FcεRI, F4/80, CD11b, CD11c, and CD49b. Sorting of IL-33–activated ILC2s and naive ILCs was performed with a FACSAria cell sorter (BD Biosciences), with a sorting purity of greater than 95%.

In vitro ILC2 and ILC culture

Freshly sorted lung ILC2s were cultured, as previously described,[E2] with modifications. Briefly, ILC2s were expanded for 6 days in RPMI 1640 supplemented with 10% FBS, IL-33, IL-2, and IL-7 (all at 10 ng/mL). Cells were rested for 3 days in complete RPMI 1640 medium supplemented with IL-2 and IL-7 (both at 10 ng/mL) before each experiment. In some experiments ILC2s were treated with AR460262 (Cayman Chemical) or 4-CMTB (Tocris Bioscience, Bristol, United Kingdom) at the indicated concentrations and time points.

For ILC culture, cells were sorted and seeded at 1.0×10^4 cells/well in 150 μL of culture medium containing IL-33 (50 ng/mL), IL-2, and IL-7 (both at 10 ng/mL) with the appropriate treatment for 5 days.

CFSE labeling

For CFSE labeling, cultured ILC2s (1.5×10^4 cells/well in 150 μL of culture medium) were incubated with 5 μmol/L CFSE for 5 days, according to the manufacturer's protocol.

Lung histology

Lungs were fixed with 4% formaldehyde (Merck, Darmstadt, Germany) and gradually dehydrated with 30%, 50%, and 70% ethanol (J.T. Baker). The lungs were embedded in paraffin and stained with hematoxylin and eosin or periodic acid–Schiff stain. Images were acquired with an Olympus CX31 microscope (Olympus, Tokyo, Japan).

Preparation of lung homogenates for ELISA

Whole lungs were minced and homogenized by means of sonication with Bioruptor Plus (Diagenode, Liège, Belgium) in protein lysis buffer (containing 20 mmol/L HEPES HCl [pH 7.4], 150 mmol/L NaCl, 1 mmol/L $CaCl_2$, 1 mmol/L $MgCl_2$, 1% NP-40, 0.5% sodium deoxycholate, 1× protease cocktail inhibitor, and 1× phosphatase inhibitors II and III). Lung lysates were obtained by means of centrifugation at 20,000*g* for 30 minutes at 4°C and quantified with the BCA Protein Assay Kit (Thermo Fisher Scientific, Waltham, Mass).

ELISA

IL-17A, IFN-γ, IL-13, and IL-5 concentrations in either the culture supernatants of murine and human ILC2s (7.5×10^4 and 1.0×10^4 cells/well, respectively, in 150 μL of culture medium in triplicates), mouse naive ILC cultures (1.0×10^4 cells/well in 150 μL of culture medium in triplicates), or lung homogenates and BALF of mice were determined by using ELISA kits from BioLegend, with the exception of mouse IL-13 (eBioscience), according to the manufacturer's instructions. Cytokine levels in lung homogenates were presented as the amount of cytokines per milligram of total lung protein.

Quantitative real-time PCR analysis

Total RNA from cultured ILC2s (1×10^6 cells/well in 1 mL of culture medium in triplicates) was extracted by using Quick-RNA MicroPrep (Zymo Research, Irvine, Clif). A total of 0.5 to 1 μg of cDNA was synthesized by using the high-capacity cDNA reverse transcription kit (Applied Biosystems, Foster City, Calif), and quantitative real-time PCR was performed on the TOptical 96 Real-Time PCR Thermal Cycler (Biometra, Göttingen, Germany). Reactions were run in triplicates, and samples were normalized to glyceraldehyde-3-phosphate dehydrogenase expression and expressed according to the $2^{-\Delta\Delta Ct}$ method.

Multiplex bead assay analysis

Phosphorylation of Akt (pS473), ERK (pT185/pY187), c-Jun N-terminal kinase (pT183/pY185), and p38 (pT180/pY182) in ILC2 culture (2×10^6 cells/well in 2 mL of culture medium) was analyzed by using the MILLIPLEX MAP kit (Millipore, Temecula, Calif), according to the manufacturer's instructions. Data were acquired on the Bioplex Suspension Array System (Bio-Rad Laboratories, Hercules, Calif) and analyzed with Bioplex Manager 6.1 software.

Immunoblot analysis

Cultured ILC2s (2×10^6 cells/well in 2 mL of culture medium) were lysed in protein lysis buffer and sonicated, and cell debris was removed by means of centrifugation at 20,000*g* for 10 minutes at 4°C. Protein concentrations were determined by using the Micro BCA Protein Assay Kit (Thermo Fisher Scientific). Equal amounts of protein (15 μg per sample) were separated by using SDS-PAGE, transferred to polyvinylidene difluoride membrane (PALL, Port Washington, NY), and blotted according to standard procedures. Membranes were blocked with Tris-buffered saline and Tween 20 containing 5% BSA. The primary antibodies used were rabbit polyclonal anti-histone H3 (CST), anti–acetyl-histone H3 (Lys9/ys14; CST), and anti-actin (Santa Cruz Biotechnology, Dallas, Tex). Polyclonal antibodies were blotted with peroxidase-conjugated anti-rabbit IgG (CST), followed by detection with Western Lightning ECL Pro Reagent (PerkinElmer, Waltham, Mass), according to the manufacturer's recommendations.

HDAC activity assay

ILC2 nuclear extracts (1×10^7 cells/well in 10 mL of culture medium) were prepared by using the Nuclei EZ Prep kit (Sigma-Aldrich) and quantified by with the Micro BCA Protein Assay Kit. HDAC activity was measured with the EpiQuik HDAC Activity/Inhibition Assay Kit (Epigentek, Farmingdale, NY), according to the manufacturer's instructions.

T_H2 polarization of OT-II cells

OT-II mice were sensitized with 10 μg of ovalbumin peptide 323-339 (pOVA; InvivoGen, San Diego, Calif) in alum (InvivoGen) for 14 days. T cells from spleens of pOVA-sensitized mice were cultured under T_H2-polarizing conditions, as previously described.[E3]

REFERENCES

E1. Kim BS, Lu H, Ichiyama K, Chen X, Zhang YB, Mistry NA, et al. Generation of RORgammat(+) antigen-specific T regulatory 17 cells from Foxp3(+) precursors in autoimmunity. Cell Rep 2017;21:195-207.

E2. Yu X, Pappu R, Ramirez-Carrozzi V, Ota N, Caplazi P, Zhang J, et al. TNF superfamily member TL1A elicits type 2 innate lymphoid cells at mucosal barriers. Mucosal Immunol 2014;7:730-40.

E3. Mackenzie KJ, Nowakowska DJ, Leech MD, McFarlane AJ, Wilson C, Fitch PM, et al. Effector and central memory T helper 2 cells respond differently to peptide immunotherapy. Proc Natl Acad Sci U S A 2014; 111:E784-93.

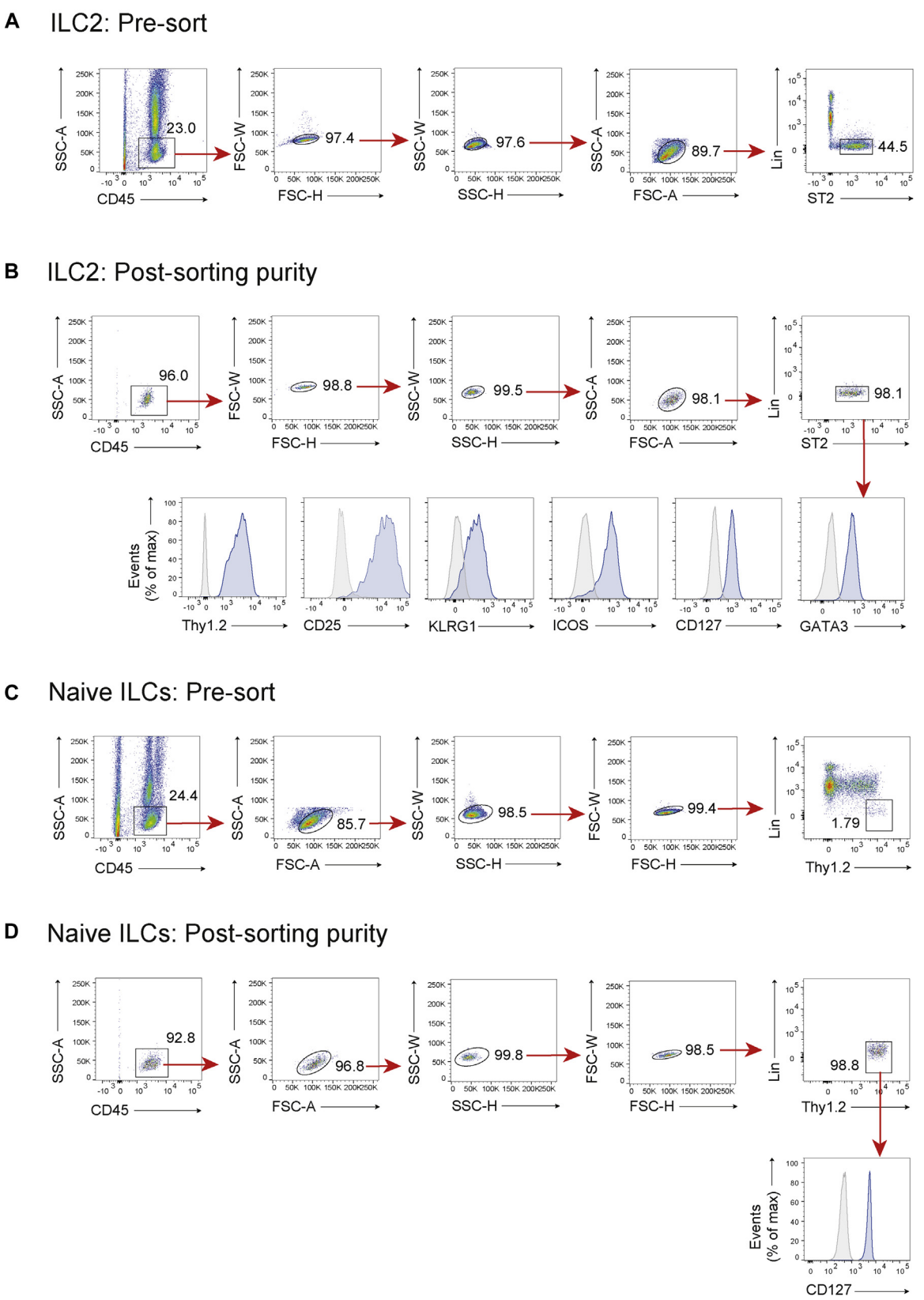

FIG E1. Murine ILC2s and naive ILC cell-sorting strategy and purity. **A,** Gating strategy for sorting lung ILC2s from *Rag2*$^{-/-}$ mice treated with IL-33 (0.1 μg) daily for 3 days and killed 3 days later. Lung ILC2s were defined as Lin^{-}CD45^{+}ST2^{+} cells. **B,** Purity and surface phenotype (Thy1.2, CD25, KLRG1, ICOS, CD127, and GATA3) of postsorted lung ILC2s. **C,** Gating strategy for sorting lung ILCs from naive *Rag2*$^{-/-}$ mice. Lung ILCs were defined as Lin^{-}CD45^{+}Thy1.2^{+} cells. **D,** Purity and CD127 expression of postsorted lung ILCs. Representative histograms are shown, whereby *gray solid lines* indicate isotype-matched control and *blue solid lines* indicate antibody staining. *FSC,* Forward scatter; *SSC,* side scatter.

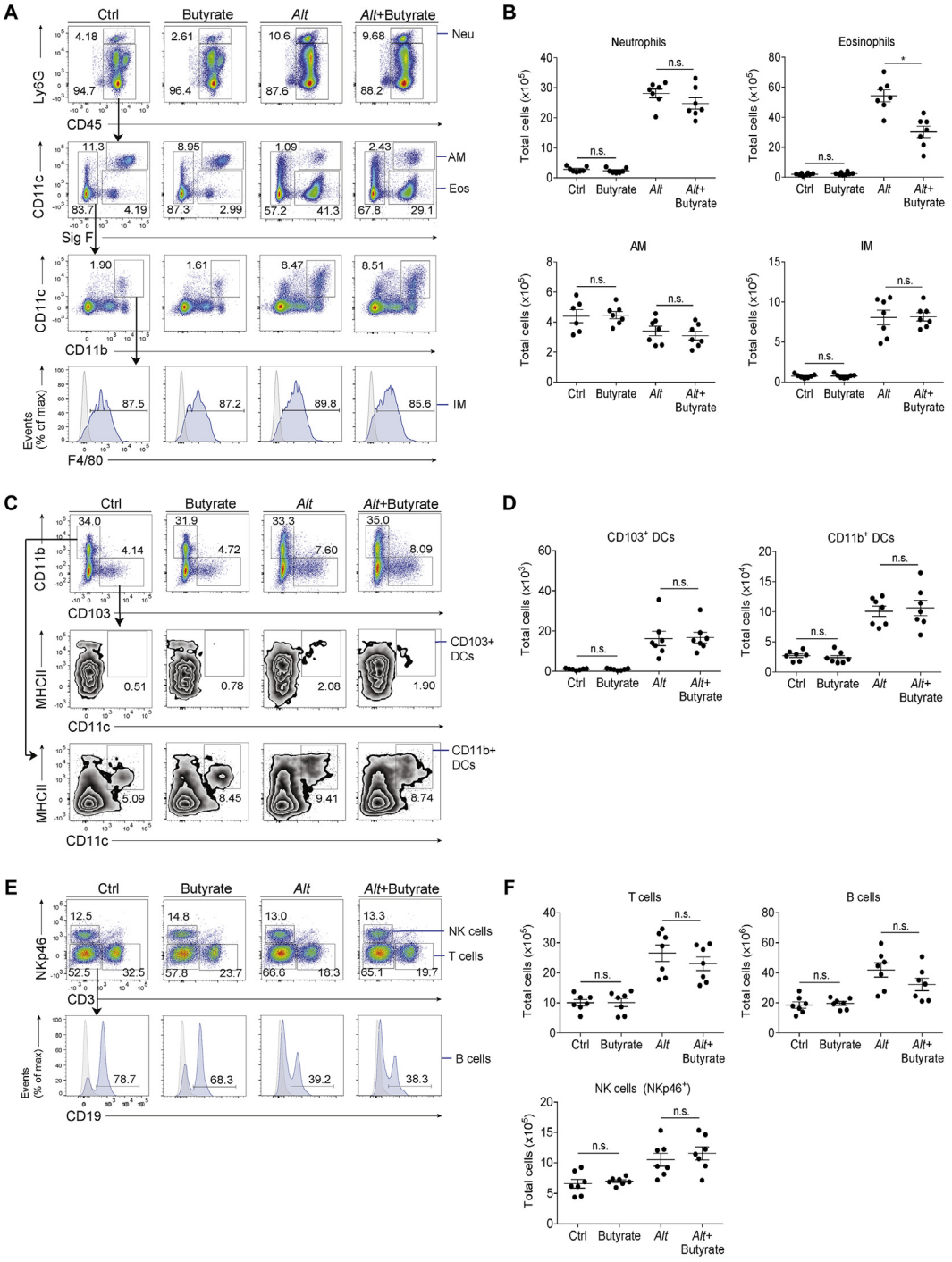

FIG E2. Myeloid and lymphoid cell distribution in lungs of *A alternata*–challenged mice after exposure to butyrate or saline in drinking water. BALB/c mice were given butyrate in drinking water for 6 weeks and challenged with *A alternata* daily for 4 days as in Fig 2, *A*, protocol 1. **A,** Gating strategy for lung neutrophils (*Neu*; $CD45^+Ly6G^+$), eosinophils (*Eos*; $CD45^+Ly6G^-Siglec\text{-}F^+CD11c^-$), alveolar macrophages (*AM*; $CD45^+Ly6G^-Siglec\text{-}F^+CD11c^+$), and interstitial macrophages (*IM*; $CD45^+Ly6G^-Siglec\text{-}F^-CD11c^+CD11b^+F4/80^+$). **B,** Total numbers of lung neutrophils, eosinophils, AMs, and IMs assessed as in Fig E2, *A*. **C,** Gating strategy for lung $CD103^+$ dendritic cells (*DCs*; $CD11b^-CD103^+CD11c^+$MHC class II^+) and $CD11b^+$ DCs ($CD11b^+CD103^-CD11c^+$MHC class II^+) gated from the viable $CD45^+Ly6G^-F4/80^-$ population. **D,** Total number of $CD103^+$ and $CD11b^+$ DCs assessed as in Fig E2, *C*. **E,** Gating strategy for lung natural killer *(NK)* cells ($CD45^+CD3^-NKp46^+$), T cells ($CD45^+CD3^+$), and B cells ($CD45^+CD3^-NKp46^-CD19^+$). **F,** Total number of lung NK, B, and T cells assessed as in Fig E2, *E*. Representative histograms are shown, whereby *gray solid lines* indicate isotype-matched control and *blue solid lines* indicate antibody staining. Data are shown as means ± SEMs from 2 independent experiments (n = 7). *n.s.*, Not significant. $*P < .05$.

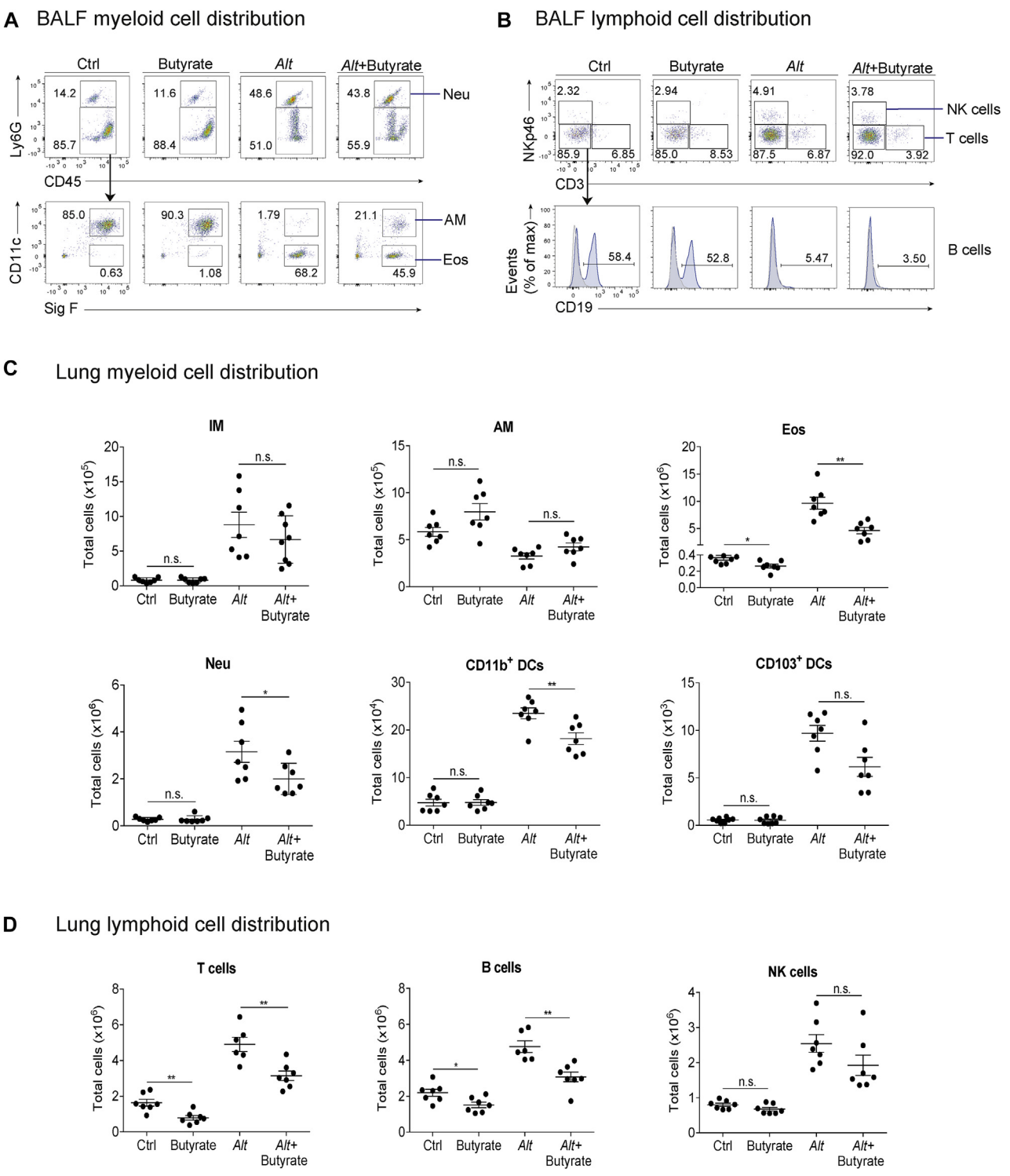

FIG E3. Myeloid and lymphoid cell distribution in BALF and lung tissue of *A alternata*–challenged mice treated intranasally with butyrate. BALB/c mice were administered intranasal butyrate before challenge with *A alternata* daily for 4 days, as in Fig 3, *A*. **A,** Representative flow diagram showing the gating strategy for BALF neutrophils (*Neu*; $CD45^+Ly6G^+$), eosinophils (*Eos*; $D45^+Ly6G^-Siglec\text{-}F^+CD11c^-$), and alveolar macrophages (*AM*; $CD45^+Ly6G^-Siglec\text{-}F^+CD11c^+$). **B,** Representative flow diagram showing the gating strategy for BALF natural killer *(NK)* cells ($CD45^+CD3^-NKp46^+$), T cells ($CD45^+CD3^+$), and B cells ($CD45^+CD3^-NKp46^-CD19^+$). **C,** Total number of lung neutrophils, eosinophils, AMs, IMs, $CD103^+$ dendritic cells *(DCs)*, and $CD11b^+$ DCs gated and assessed as in Fig E2, *A* (neutrophils, eosinophils, AMs, and IMs) and Fig E2, *C* ($CD103^+$ and $CD11b^+$ DCs). **D,** Total number of lung NK, B, and T cells gated and assessed as in Fig E2, *E*. Representative histograms are shown, whereby *gray solid lines* indicate isotype-matched control and *blue solid lines* indicate antibody staining. Data are shown as means ± SEMs from 2 independent experiments (n = 7). *n.s.*, Not significant. $*P < .05$ and $**P < .01$.

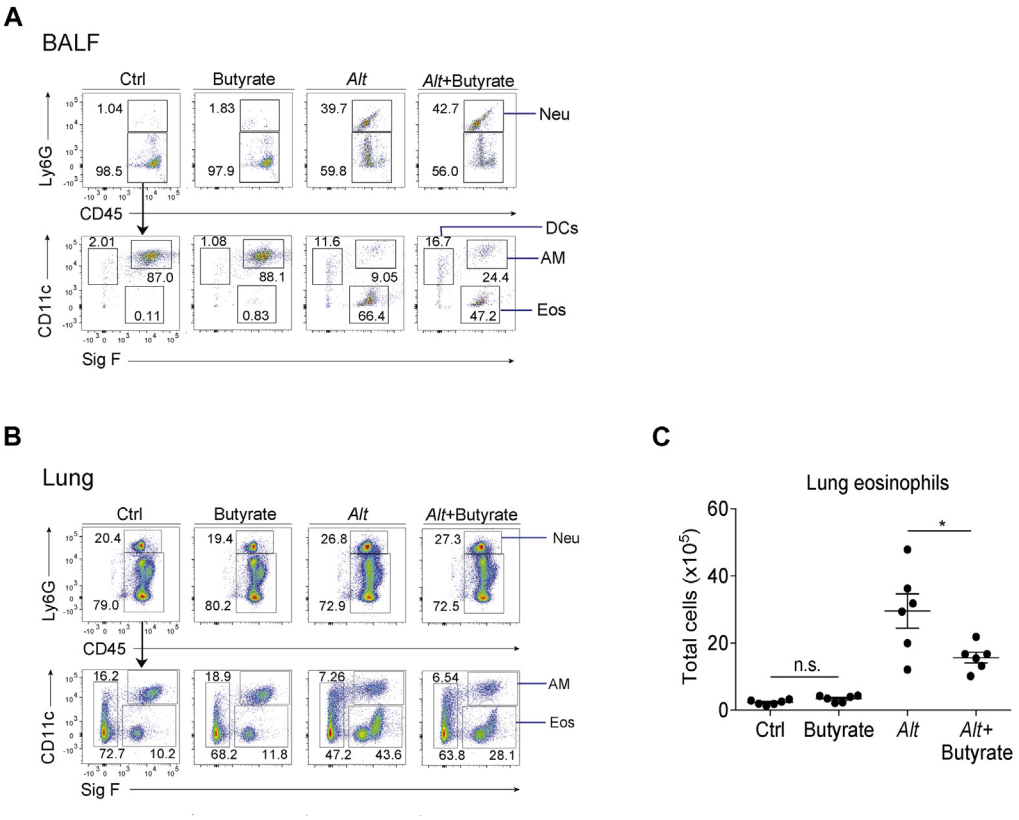

FIG E4. Intranasal administration of butyrate inhibits *A alternata*–induced eosinophilia in *Rag2*$^{-/-}$ mice. *Rag2*$^{-/-}$ mice were treated as in Fig 3, *A*. **A** and **B,** Representative flow diagram showing the gating strategy for neutrophils, (*Neu*; CD45^{+}Ly6G^{+}), eosinophils (*Eos*; CD45^{+}Ly6G^{-}Siglec-F^{+}CD11c^{-}), and alveolar macrophages (*AM*; CD45^{+}Ly6G^{-}Siglec-F^{+}CD11c^{+}) in the BALF (Fig E4, *A*) and lungs (Fig E4, *B*). **C,** Total lung eosinophils assessed as in Fig E4, *B*. Data are shown as means ± SEMs from 2 independent experiments (n = 7). *n.s.*, Not significant. **P* < .05.

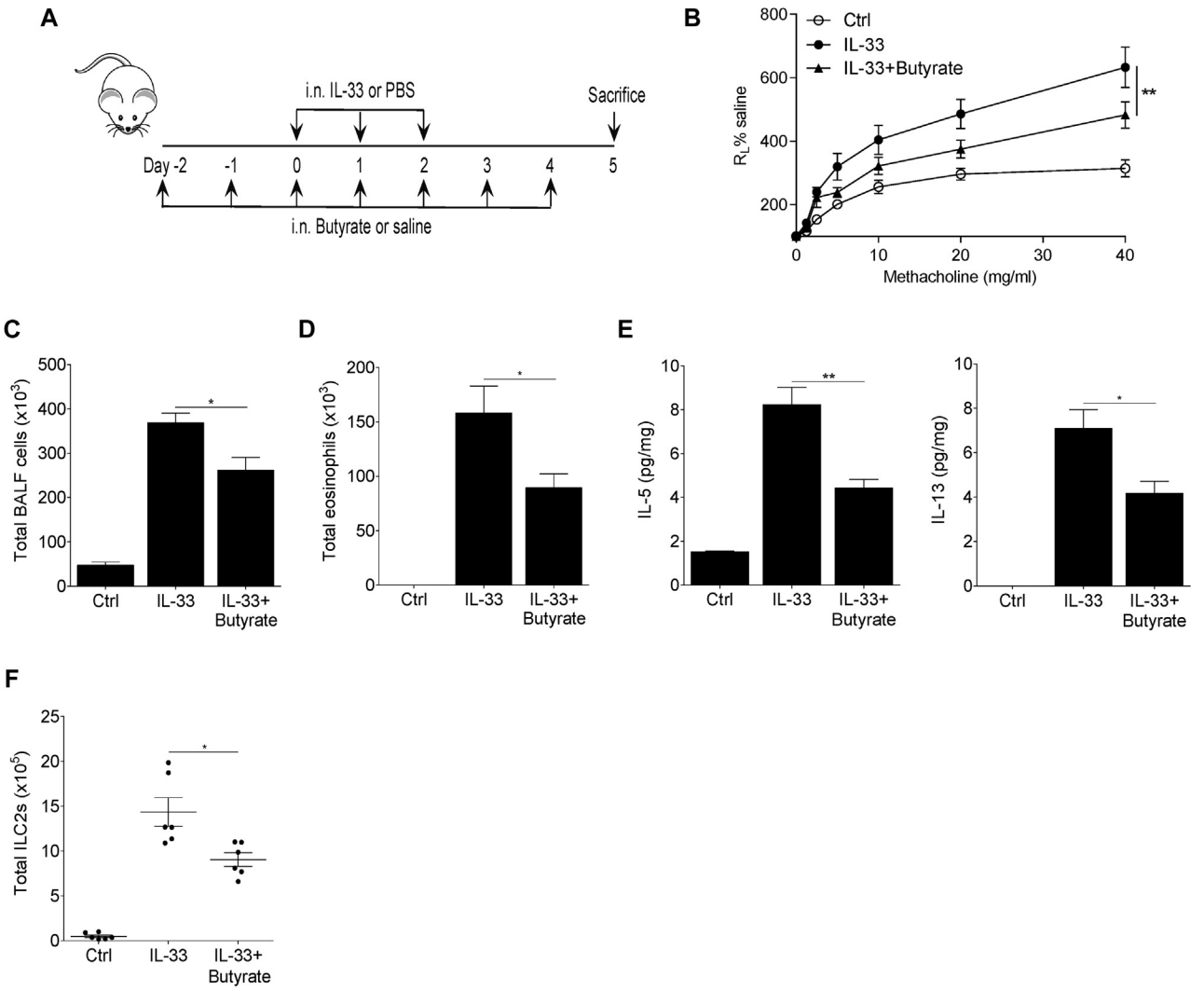

FIG E5. Intranasal administration of butyrate prevents IL-33–induced type 2 inflammation. **A,** Schematic diagram of butyrate treatment by means of intranasal *(i.n.)* delivery in an IL-33 model of airway inflammation in BALB/c mice. **B,** Lung resistance in response to increasing doses of methacholine. **C** and **D,** Total cells (Fig E5, *C*) and eosinophils (Fig E5, *D*) in BALF. **E,** IL-5 and IL-13 levels in lung homogenates of mice. **F,** Total number of lung ILC2s per mouse. Data are shown as means ± SEMs of 2 independent experiments (n = 6 each). $*P < .05$ and $**P < .01$.

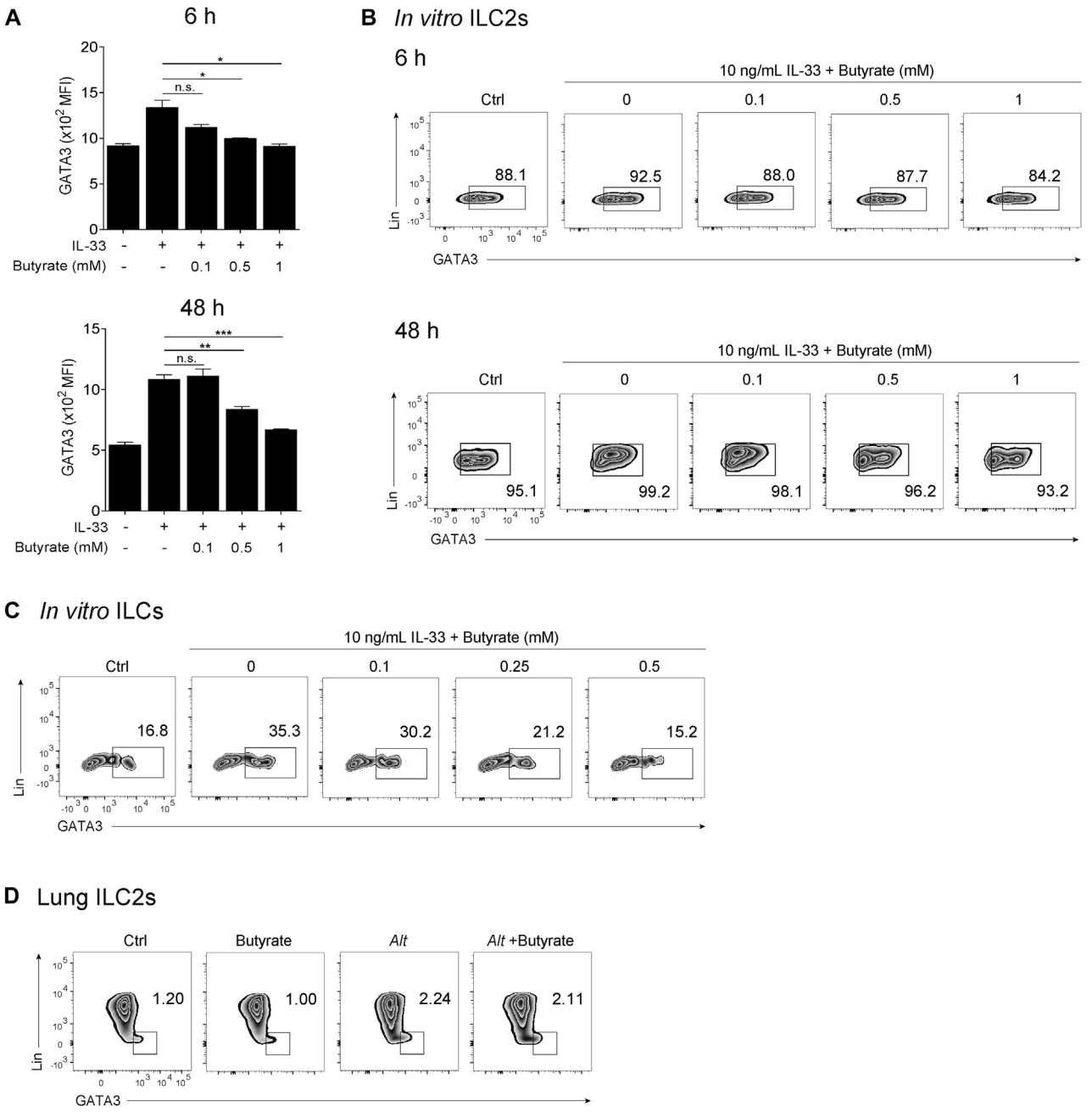

FIG E6. Butyrate treatment reduces GATA3 expression in ILC2s. **A** and **B,** Lung ILC2s were sorted from IL-33–treated *Rag2*$^{-/-}$ mice and treated with IL-33, IL-2, and IL-7 (all at 10 ng/mL) in the absence or presence of butyrate at the indicated concentrations. Control cells were cultured with IL-2 and IL-7 (both at 10 ng/mL) only. Fig E6, *A*, Mean fluorescence intensity *(MFI)* of GATA3 after 6 or 48 hours of treatment assessed as in Fig 5, *E*. Data are shown as means ± SDs from 1 of 2 independent experiments (n = 3 wells) with consistent findings. *n.s.*, Not significant. **P* < .05, ***P* < .01, and ****P* < .0001. Fig E6, *B*, Representative flow diagram showing Lin$^-$GATA3$^+$ ILC2s after treatment for 6 or 48 hours gated from viable CD45$^+$ cells. **C,** Total ILCs were cultured with IL-33 (50 ng/mL), IL-2, and IL-7 (both at 10 ng/mL) in the presence or absence of butyrate at the indicated concentrations for 5 days. Control cells were cultured with IL-2 and IL-7 only (both at 10 ng/mL). Lin$^-$GATA3$^+$ ILC2s were gated from viable CD45$^+$ cells. **D,** BALB/c mice were treated with butyrate and *A alternata* according to the protocol in Fig 3, *A*. Lin$^-$GATA3$^+$ ILC2s were gated from a viable forward scatter–low/side scatter–low CD45$^+$TCRβ$^-$B220$^-$ population.

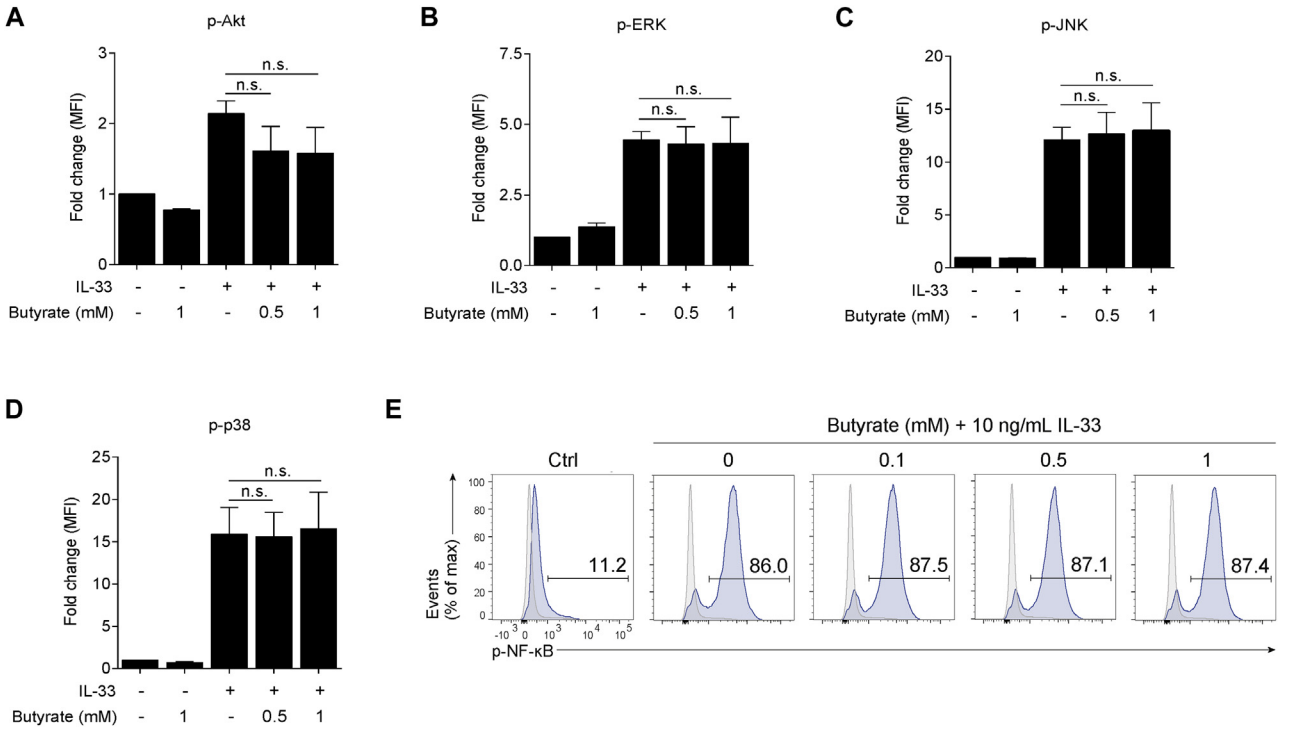

FIG E7. Butyrate does not affect signaling pathways downstream of IL-33/ST2 receptor. Sorted lung ILC2s were cultured with IL-33, IL-2, and IL-7 (all at 10 ng/mL) with or without butyrate at indicated concentrations for 10 minutes. Control cells were cultured with IL-2 and IL-7 only (both at 10 ng/mL). **A-D,** Multiplex bead array analysis of the phosphorylated form of Akt (Fig E7, *A*), ERK (Fig E7, *B*), c-Jun N-terminal kinase (*JNK*; Fig E7, *C*), and p38 (Fig E7, *D*). **E,** Flow cytometry of phospho–NF-κB. Data are shown as means ± SDs from 1 of 2 independent experiments (n = 3 wells) with consistent findings. *n.s.*, Not significant.

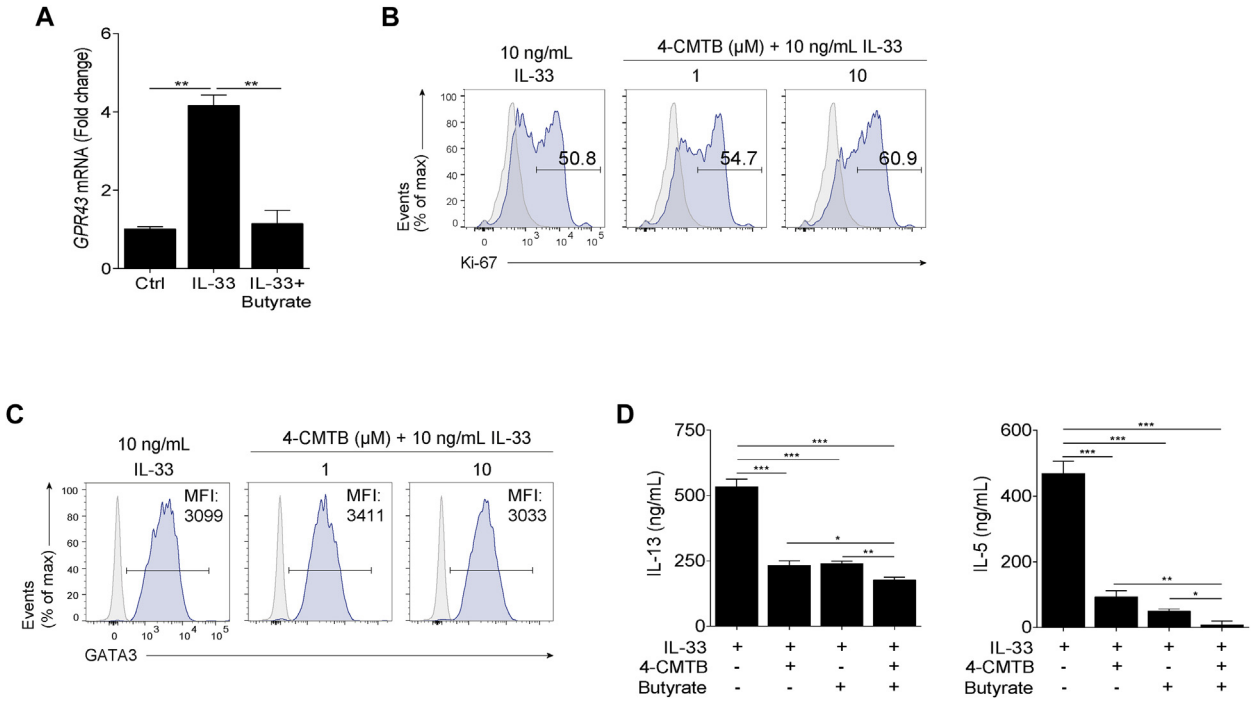

FIG E8. Butyrate-mediated inhibition is independent of GPR43. ILC2s were sorted from the lungs of IL-33–treated *Rag2*$^{-/-}$ mice and cultured with IL-33, IL-2, and IL-7 (all at 10 ng/mL) in the presence or absence of butyrate, 4-CMTB, or both at the indicated concentrations. Control cells were cultured with IL-2 and IL-7 only (both at 10 ng/mL). **A,** *GPR43* mRNA expression after 6 hours of treatment with IL-33 in the presence or absence of 1 mmol/L butyrate. **B,** Proliferation of ILC2s, as assessed based on Ki-67 after 48 hours of treatment. **C,** Mean fluorescence intensity *(MFI)* of GATA3 in ILC2s after treatment for 48 hours. Representative histograms are shown, whereby *gray solid lines* indicate isotype-matched control and *blue solid lines* indicate antibody staining. **D,** IL-13 and IL-5 levels in culture supernatants of ILC2s after 48 hours of treatment with 5 μmol/L 4-CMTB, 0.5 mmol/L butyrate, or both in the presence of IL-33 (10 ng/mL). Data are shown as means ± SDs from 1 of 2 independent experiments (n = 3 wells) with consistent findings. **P* < .05, ***P* < .01, and ****P* < .001.

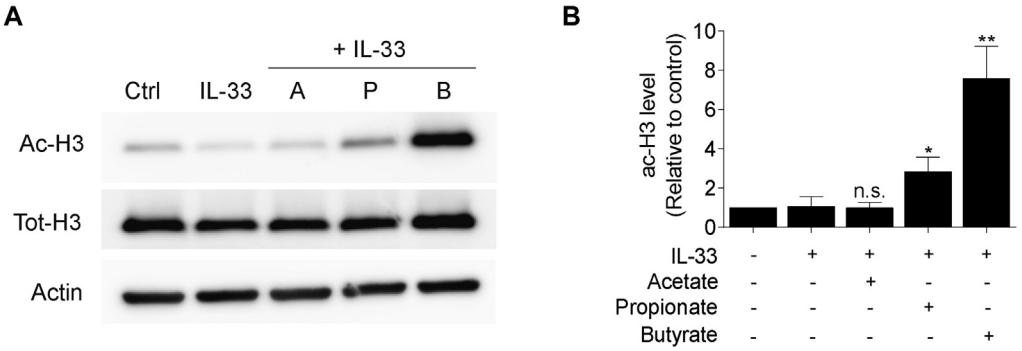

FIG E9. Propionate is a weaker inducer of H3 acetylation than butyrate. Sorted lung ILC2s were cultured with IL-33, IL-2, and IL-7 (all at 10 ng/mL) in the absence or presence of acetate *(A)*, propionate *(P)*, or butyrate (*B*; all at 1 mmol/L) for 6 hours. Control cells were cultured with IL-2 and IL-7 only (both at 10 ng/mL). Representative Western blot image **(A)** and relative expression **(B)** of ac-H3 levels are shown. Data were normalized against total H3. Data are shown as means ± SDs from 3 independent experiments. *n.s.*, Not significant. **P* < .05 and ***P* < .01 (compared with the IL-33–treated group).

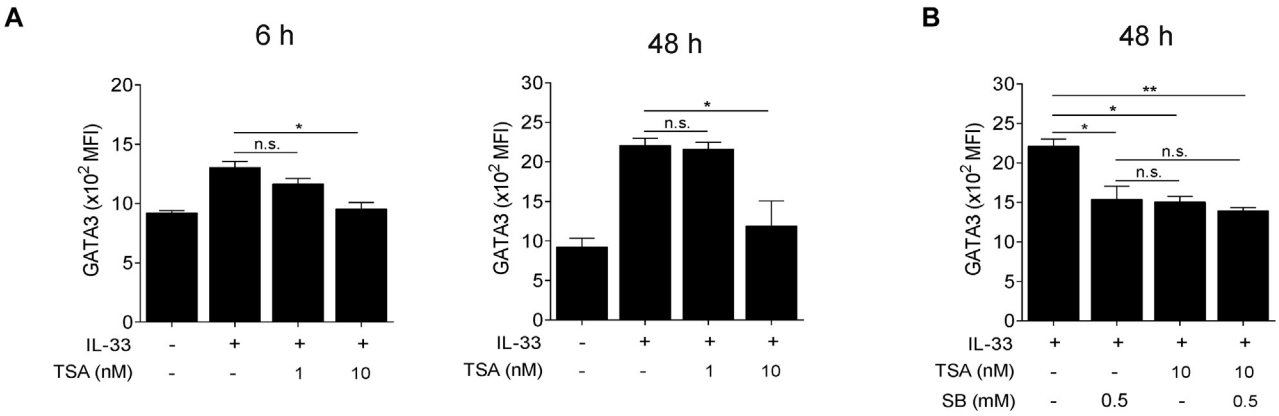

FIG E10. TSA inhibits GATA3 expression. Sorted lung ILC2s were cultured with IL-33, IL-2, and IL-7 (all at 10 ng/mL) in the absence or presence of TSA, butyrate, or both at the indicated concentrations. Control cells were cultured with IL-2 and IL-7 only (both at 10 ng/mL). **A,** Mean fluorescence intensity *(MFI)* of GATA3 after 6 or 48 hours of treatment assessed as in Fig 7, *G*. **B,** MFI of GATA3 after 48 hours of treatment, assessed as in Fig 7, *J*. Data are shown as means ± SDs from 1 of 2 independent experiments (n = 3 wells) with consistent findings. *n.s.*, Not significant. **P* < .05, ***P* < .01, and ****P* < .001.